PERGAMON

Journal of Structural Geology 25 (2003) 1171–1192

JOURNAL OF STRUCTURAL GEOLOGY

www.elsevier.com/locate/jsg

Mechanical stratigraphy and fault–fold interaction, Absaroka thrust sheet, Salt River Range, Wyoming

Judith S. Chester*

Center for Tectonophysics and Department of Geology and Geophysics, Texas A & M University, College Station, TX 77843, USA

Received 11 August 2000; received in revised form 31 July 2002; accepted 21 August 2002

Abstract

A distinct contrast in deformation style from tightly folded and faulted Cambrian through Ordovician strata to broadly folded and faulted Mississippian and younger strata is displayed in the hanging wall of the Absaroka thrust, Salt River Range, Wyoming. Based on style, the Paleozoic section can be divided into two main structural lithic units. Each unit is characterized by a relatively weak, ductile, anisotropic lower section and a relatively strong, brittle, more isotropic upper section. Where the two units were stacked within the thrust sheet, inverted fault–propagation folds formed in the center of each unit, and the overall transition upward from close- to wide-spaced folds and imbricate faults developed in the multilayer. Where the upper unit was isolated, deformation was dominated by imbricate faulting with little associated folding, and inverted fault–propagation folds did not form. Observations illustrate that the mechanical interaction between the two units and boundary conditions imposed on them were significant to defining the deformation response. It is note-worthy that the boundary between the two structural lithic unts, in part defined by the roof thrust of the Stewart passive roof duplex, occurs within a dolostone rather than in overlying shale of the Darby Formation. I propose that the roof thrust and other detachments in dolostone reflect the relatively low frictional strength of dolostone under shallow crustal conditions. Cross-cutting relations suggest that the Absaroka sheet was cut by large imbricate faults during late-stage movement over a major dip ramp. A high deviatoric and low mean compressive stress state just beyond the upper ramp–flat corner promoted break-back imbrication and allowed tectonic thickening of the thrust wedge necessary to reestablish critical taper and for forward translation.

Keywords: Mechanical stratigraphy; Fault–fold interaction; Multilayer deformation; Wedge mechanics; Duplex

1. Introduction

Analysis of thin-skinned fold-and-thrust belts as deformable, sliding wedges provides a mechanical framework to understand deformation and translation of thrust sheets (e.g. Davis et al., 1983). In general, fold-and-thrust belts display a hinterland to foreland sequence of deformation superposed with episodes of out-of-sequence and hinterland verging thrusting events (e.g. Armstrong and Oriel, 1965; Royse et al., 1975; Lamerson, 1982; Wiltschko and Dorr, 1983; Schirmer, 1988; Yonkee, 1992; DeCelles and Mitra, 1995; Mitra and Sussman, 1997). Thickening in the hinterland potion of the wedge by out-of-sequence deformation can be achieved by a variety of mechanisms (e.g. Mitra and Sussman, 1997) and may be necessary to maintain critical wedge taper for continued sliding.

Homogeneous mechanical properties and distributed deformation are general assumptions of models of critically-tapered wedges. Although these assumptions may be appropriate for an entire thrust belt, individual fold-and-thrust systems consist of discrete thrust sheets and duplex systems that are displaced along irregular (stepped) fault surfaces (e.g. Rich, 1934; Douglas, 1950; Royse et al., 1975; Boyer and Elliot, 1982). Deformation within a thrust sheet characteristically is heterogeneous in space and episodic in time (e.g. Wiltschko and Dorr, 1983; Coogan, 1992) as a result of fault–fold interaction at a variety of scales. Mechanical models of thrust sheet movement over stepped and curved fault surfaces to produce ramp-related folds illustrate that a variety of parameters influence the kinematics of deformation, including geometry and mechanical properties of layering (e.g. Raleigh and Griggs, 1963; Elliot, 1976; Wiltschko, 1979; Berger and Johnson, 1980; Kilsdonk and Fletcher, 1989; Erickson and Jamison, 1995;

* Fax: +1-979-845-1380.
E-mail address: chesterj@geo.tamu.edu (J.S. Chester).

0191-8141/03/$ - see front matter
PII: S0191-8141(02)00151-7

Jamison, 1996; Chester and Fletcher, 1997; Strayer and Hudleston, 1997; Erickson et al., 2001).

The influence of stratigraphic layering on fold geometry and mechanics was first treated in terms of competence contrasts and the concept of passive and active layers (Willis, 1894). Competent horizons support layer-parallel stresses, transmit loads over great distances, and are able to buckle. Incompetent horizons offer no appreciable resistance to bending and thicken by flow in response to applied loads. Experimental and theoretical mechanics analysis of buckling led to the recognition that an individual, dominant member of a multilayer could control fold wavelength, but that strata consisting of many competent and incompetent layers of variable thicknesses tend to develop complex fold geometries (Currie et al., 1962). Expanding on the concept of a dominant member, Currie et al. (1962) suggested that a specific portion of a multilayer that displays a characteristic reaction to deformation be defined as a structural lithic unit. Donath and Parker (1964) emphasized the need to describe the overall behavior of a structural lithic unit in terms of well-defined mechanical properties, such as ductility contrast and mean ductility. Although subsequent mechanical analyses have improved our understanding of the influence of layering, interface properties, and boundary conditions on the mechanisms of folding and resultant fold geometries (e.g. Biot, 1964, 1965a,b; Johnson, 1970, 1977; Ramberg, 1970; Cobbold et al., 1971; Latham, 1985a,b; Johnson and Fletcher, 1994), the concepts of structural lithic units (Currie et al., 1962) and mechanical characterizations of strata (Donath and Parker, 1964) continue to be useful for the analysis and prediction of natural deformation behavior (e.g. Corbett et al., 1987; Chester, 1987, 1992; Woodward, 1988, 1992; Woodward and Rutherford, 1989; Gross, 1995; Gross et al., 1997; Fischer and Jackson, 1999).

An excellent example of fault–fold interaction and heterogeneous deformation in a mechanically layered thrust sheet is displayed within the hanging wall of the Absaroka thrust, Sevier Belt, Wyoming (Fig. 1). In the Haystack Peak area, northern Salt River Range, major folds within the Absaroka sheet plunge southward over a transversely dipping portion of the Absaroka thrust providing a down-plunge view of deep and shallow structural levels (Fig. 2). Previous mapping of the Absaroka sheet (Rubey, 1973) documents a distinct contrast in deformational style from tightly folded and faulted Cambrian through Ordovician strata in the north to broadly folded and faulted Mississippian and younger strata to the south. The change in structural style has been attributed to numerous causes including a decrease in shortening of the sheet from north to south, a decrease in shortening from lower to higher structural level, presence of a detachment horizon, or a mechanical stratigraphic influence (e.g. Rubey, 1973; Royse et al., 1975; Dixon, 1982; Lageson, 1984; Woodward, 1992).

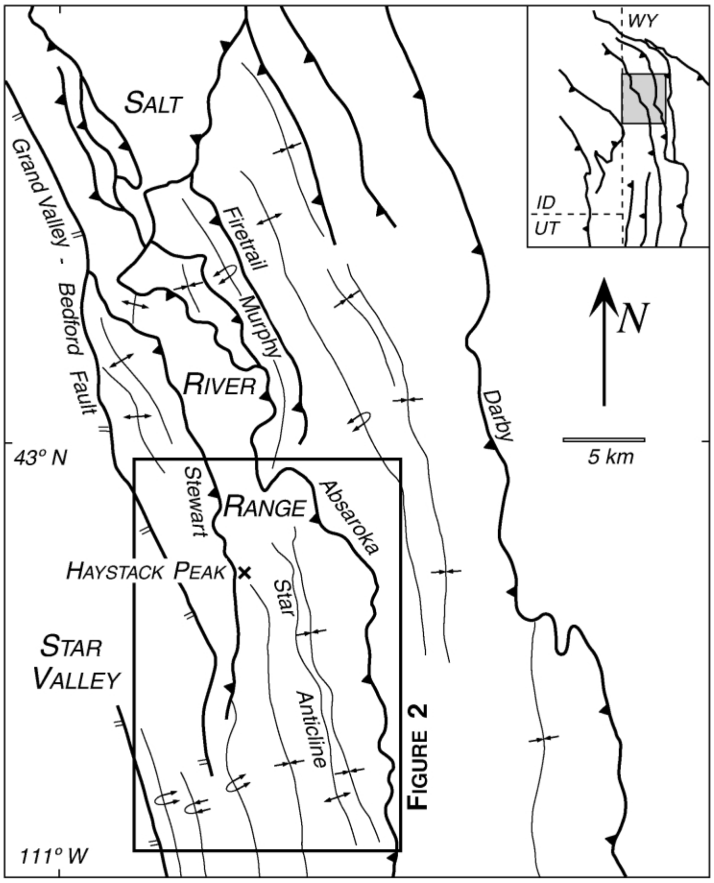

Fig. 1. Map of a portion of the Wyoming Salient, central Salt River Range, Wyoming.

The purpose of this paper is to characterize in detail the 3-D structure of the Absaroka thurst sheet in the vicinity of Haystack Peak in order to determine the geometry of the Absaroka thust, variation in shortening from north to south, and influence of the strata on structural style. I infer the mechanical properties of the stratigraphic section using published rock mechanics data and identify structural lithic units on the basis of deformation style throughout the study area. Comparison of the inferred mechanical properties with the structural lithic units provides a better understanding of the mechanical effects of stratigraphy and layering on deformation. These data are used to better constrain the kinematics of this portion of the thrust sheet.

2. Geologic background

2.1. Structure

The Idaho–Wyoming–northern Utah Salient of the Sevier belt is cut by six major thrust faults (e.g. Armstrong and Oriel, 1965; Royse et al., 1975; Wiltschko and Dorr, 1983; Elison, 1991; Coogan, 1992). The Absaroka thrust, which is the third youngest major fault, was active from 62 to 84 Ma in the southern part of the belt (Lamerson, 1982; Wiltschko and Dorr, 1983; Elison, 1991; DeCelles and Mitra, 1995). Palinspastic reconstructions suggest that approximately 40 km of shortening in this portion of the Salient was accommodated by translation along the Absaroka fault surface and another 40 km by internal shortening of the Absaroka sheet (Dixon, 1982).

In the Salt River Range, the Absaroka thrust juxtaposes Cambrian–Ordovician strata in the hanging wall and Cretaceous strata in the footwall (Fig. 2; Rubey, 1973). Just west of the range the Absaroka thrust forms a large footwall dip-ramp (Grand Valley ramp) that cuts Mesozoic and Paleozoic strata to join the basal decollement of the belt (Royse et al., 1975; Dixon, 1982). This study focuses on a portion of the Absaroka thrust sheet in the Haystack Peak region, central Salt River Range, Wyoming, at the southern end of the Stewart Peak Culmination (Lageson, 1984; Woodward, 1986, 1987). Here structures plunge to the south exposing a distinct change in structural style at the surface from tightly folded and faulted Cambrian through Ordovician strata to broadly folded and faulted Mississippian and younger strata (Fig. 2; Rubey, 1973). The depth to the Absaroka fault is shown as increasing to the south in most subsurface interpretations (e.g. Rubey, 1973; Dixon, 1982; Woodward, 1987) consistent with the presence of a structural culmination; however, different fault surface shapes and cut-off angles have been presented. Dixon (1982) and Woodward (1987) suggest that the Absaroka thrust fault is transversely dipping below the Haystack Peak region. The origin of the transverse dip is uncertain, but could reflect the presence of a footwall transverse ramp in the Darby thrust (e.g. Woodward, 1987), or warping of the

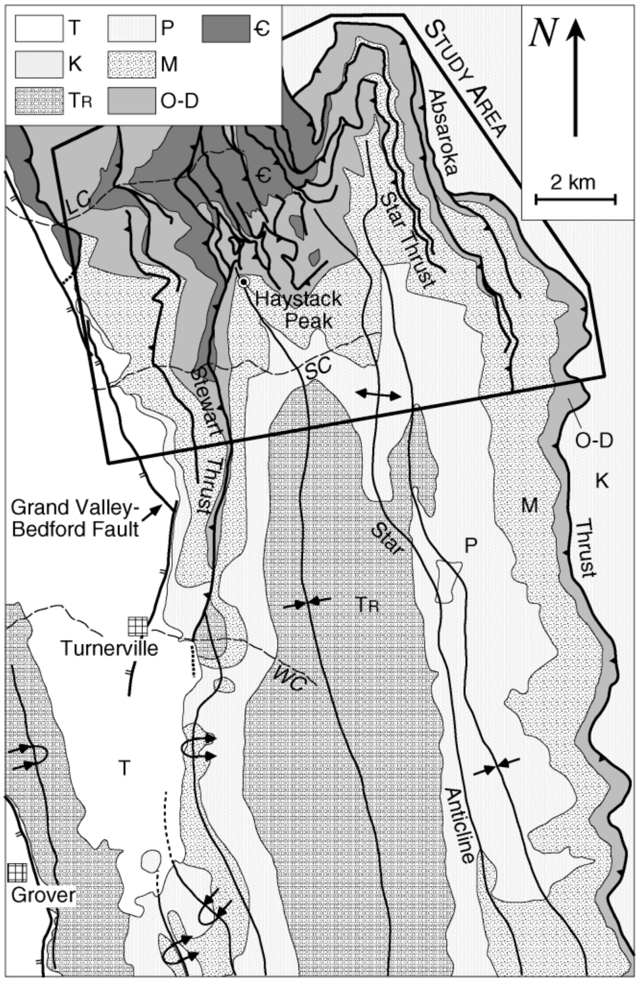

Fig. 2. Simplified geologic map of the Absaroka thrust sheet in the central Salt River Range, Wyoming showing the transition from faulting in the north to broad folding in the south, and the study area. Map modified from Chester (1996). Geographic locations shown are: Lost Creek, LC; Strawberry Creek, SC; Willow Creek, WC; Haystack Peak, HP.

Absaroka fault surface associated with movement on the southern extension of the Murphy–Firetrail fault system (e.g. Lageson, 1984). Dixon (1982) suggests that the slip distribution on the Absaroka thrust changes along strike in this region; however, Woodward (1987) argues that slip is constant. Shallow seismic reflection data generally are of poor quality in this area, and details of fault plane structure largely have been inferred from surface data and regional cross-section balancing (e.g. Dixon, 1982; Webel, 1987). The cause for the variation in structural style displayed at the surface, subsurface structure, depth to the Absaroka thrust fault, relation to the Stewart Peak culmination, and timing of imbrication within this region remain uncertain.

2.2. Stratigraphy

Portions of six formations are exposed in the Haystack Peak area between the Absaroka thrust and Grand Valley

Table 1
Lithologic description of units. Descriptions indicated by * are from Wanless et al. (1955)

Formation	Member	Rock type	Layer definition	Contact character
Mission Canyon		Interbedded bioclastic and oolitic, coarsely crystalline limestone and finely crystalline dolomite and dolomitic limestone. Upper portion is a collapse breccia of limestone, sandstone and dolomite.	Layering is defined by variations in rock type and major, planar parting surfaces. At mesoscopic scale, layering is defined by continuous parting and styolitic surfaces that are spaced 30 cm to 3 m, averaging 1 m.	The breccia forms a distinct and sharp contact with the Darwin Sandstone of the Amsden Fm. and an irregular and gradational contact with the rest of the underlying Mission Canyon Fm.
Lodgepole	Woodhurst	Very thin-bedded, finely crystalline or bioclastic limestone with argillaceous–dolomitic interlayers.	Homogenous with respect to lithology and layer thickness. Layering defined by lithologic contrast, and less often by local concentrations of styolitic surfaces that merge with argillaceous horizons.	Upper contact is abrupt and distinct lithologic, layer thickness, and layer character boundary.
	Payne	Thin-bedded, finely crystalline, blue-gray, silty and argillaceous limestone with lenticular and nodular chert horizons scattered throughout.	Homogenous with respect to lithology and layer thickness. Layering defined by local concentrations of wavy, styolitic surfaces often defined by clay seams.	Upper contact is abrupt and distinct layer boundary.
Darby	Unit 4	Interbedded yellow-brown and purplish-red calcareous siltstone and mudstone.	Bedding for entire formation is defined by sharp lithologic contrasts. Within siltstone–mudstone, layering is defined by moderately to poorly-developed fissility and planar to wavy parting. Within limestone–dolomite, layering is defined by single, continuous to discontinuous, well-developed, planar to sutured styolitic surfaces and occasionally by discontinuous, argillaceous–dolomitic or –calcareous stringers. Styolitic surfaces are spaced 30–60 cm in some sections; other sections display massive layers up to 30 m thick. These latter sections contain numerous wide-spaced, discontinuous styolitic horizons throughout.	Upper contact and those between units are abrupt and distinct.
	Unit 3	Thick-bedded brownish-gray, cavernous dolomitic limestone.		
	Unit 2	Thin-bedded to laminated yellow and purplish-red calcareous to dolomitic siltstones and mudstones.		
	Unit 1	Predominantely gray to dark-brown, nodular, interbedded dolomite and limestone.		

fault: the Gros Ventre, Gallatin, Bighorn, Darby, Lodgepole and Mission Canyon (Table 1). The Gros Ventre Formation is divided into three members, which in ascending order are the Wolsey Shale, Death Canyon Member and Park Shale. The Park Shale consists of interbedded shale and dolomitic limestone (Lageson, 1978). The Gallatin Formation is composed of thinly-bedded, micritic and bioclastic limestone mottled with silty dolomite. The Bighorn Dolomite primarily is a massive to thick-bedded dolomite. The Darby Formation is divided into four sub-units, which in ascending order are: predominantly nodular, interbedded dolomite and limestone; thin-bedded to laminated calcareous to dolomitic siltstone and mudstone; thick-bedded cavernous dolomitic limestone; and interbedded calcareous siltstone and mudstone (Lageson, 1980; Wanless et al., 1955). The Lodgepole and Mission Canyon Formations form the Madison Group. The Lodgepole Formation is composed of the Payne Member, a thin-bedded, finely crystalline, silty and argillaceous limestone containing lenticular and nodular chert horizons scattered throughout, and the Woodhurst Member, a very thin-bedded, finely-crystalline or bioclastic limestone with argillaceous–dolomitic interlayers. The Mission Canyon Formation is an interbedded bioclastic and oolitic, coarsely crystalline limestone and finely-crystalline dolomite and dolomitic limestone (e.g. Wanless et al., 1955; Budai et al., 1987). The upper portion of the Mission Canyon Formation is a collapse breccia of limestone, sandstone, and dolostone (Wanless et al., 1955).

3. Mechanical characterization of the stratigraphic section

The mechanical properties of Paleozoic strata in the Absaroka thrust sheet were inferred on the basis of detailed stratigraphic columns measured in the study area at locations that display the least penetrative strain and most continuous exposure (Chester, 1987, 1992), and published

Table 1 (*continued*)

Formation	Member	Rock type	Layer definition	Contact character
Bighorn Dolomite		Homogenous with respect to lithology and layer character, but not layer thickness.	Layering defined by single, continuous, well-developed planar to sutured styolitic surfaces and less often by local concentrations of discontinuous styolitic surfaces. Thickness ranges from 2 cm up to 30 m. Thickest beds located at top near contact with Darby. Average bed thickness is 1 m. Beds of similar thickness occur in sets that are laterally continuous, even though particular styolitic horizons are often discontinuous.	
Gallatin		Homogenous with respect to lithology and layer thickness. Thinly-bedded, micritic and bioclastic limestone mottled with yellow-orange silty dolomite. Similar to some sections of Gros Ventre, particularly the Death Canyon Member.	Layering defined by buff-weathering, silty dolomitic stringers that range from 1 cm to less than 1 mm in thickness. Upper 4 m is thicker-bedded.	At mesoscopic scale, contact with Bighorn Dolomite is distinct boundary with respect to bedding thickness and lithology.
Gros Ventre	Park Shale	Lower portion consists of $\sim$13 m gray-green shale bounded above and below by sections of thinly-bedded limestone, each of which is $\sim$6 m thick.	Heterogenous with respect to lithology and layer thickness. Layering defined by sharp and laterally continuous lithologic contrast between the limestone and shale. Shale bedding defined primarily by fissility and to a lesser degree by thin, lenticular limestone layers that average 1 cm in thickness.	
	Death Canyon	Two sections of medium- to thick-bedded, dull blue-gray limestone separated by fossiliferous shale. Limestone is mottled with irregular discontinuous patches of yellow-orange, silty dolomite, which form irregular wavy, well-defined, generally planar bedding surfaces at the macroscopic scale.*		
	Wolsey Shale	Light olive-gray, flakey shale, and interbedded limestone and mottled dolomitic limestone.*		

experimental rock deformation data for analogous rock types (Handin et al., 1963; Handin, 1969). The stratigraphic columns emphasize intrinsic rock parameters important to mechanical properties, i.e. lithologic characteristics including main layer rock type and interlayer rock type, bedding thickness, interlayer thickness, character of bedding planes, and lateral continuity of bedding (Table 1 and Fig. 3).

Experimental rock deformation data were used to infer fracture or yield strength, relative ductility, and frictional strength of each unit (Fig. 4). Because deformation experiments used as analogs for the Paleozoic strata were conducted at relatively high strain rates and low temperatures one must consider the influence of strain rate and temperature when applying these data to the Absaroka thrust sheet. Assuming a maximum thickness of the Absaroka thrust sheet of approximately 5 km (Budai and Wiltschko, 1987), a normal geotherm, hydrostatic pore pressure, and no overlying thrust sheet, the temperature during deformation was approximately 120 °C and effective confining pressure was approximately 75 MPa. Although experimental rock deformation data are available for many sedimentary rock types at these pressures and temperatures, laboratory strain rates are much greater than natural strain rates. In general, the lower strain rate of natural deformation tends to promote time-dependent mechanisms such as subcritical cracking, pressure solution, and intracrystalline plasticity (e.g. Heard, 1963; Rutter, 1976, 1983; Atkinson, 1984), which would lower the strength and increase the ductility of limestone and shale relative to dolomite and quartz sandstone.

The degree of strength anisotropy considers three parameters equally: ductility contrast between the rock-type of the main layer relative to interlayer material, if present; thickness of layers; and type and continuity of bedding (Table 1 and Fig. 3). The ductility contrast parameter describes the main layer lithology relative to interlayer lithology based on data of Handin et al. (1963) and concepts of Donath and Parker (1964). The layer thickness parameter ranks the thinnest layering as the most anisotropic. The bedding parameter is subdivided into three groups that reflect type and continuity of layer-parallel

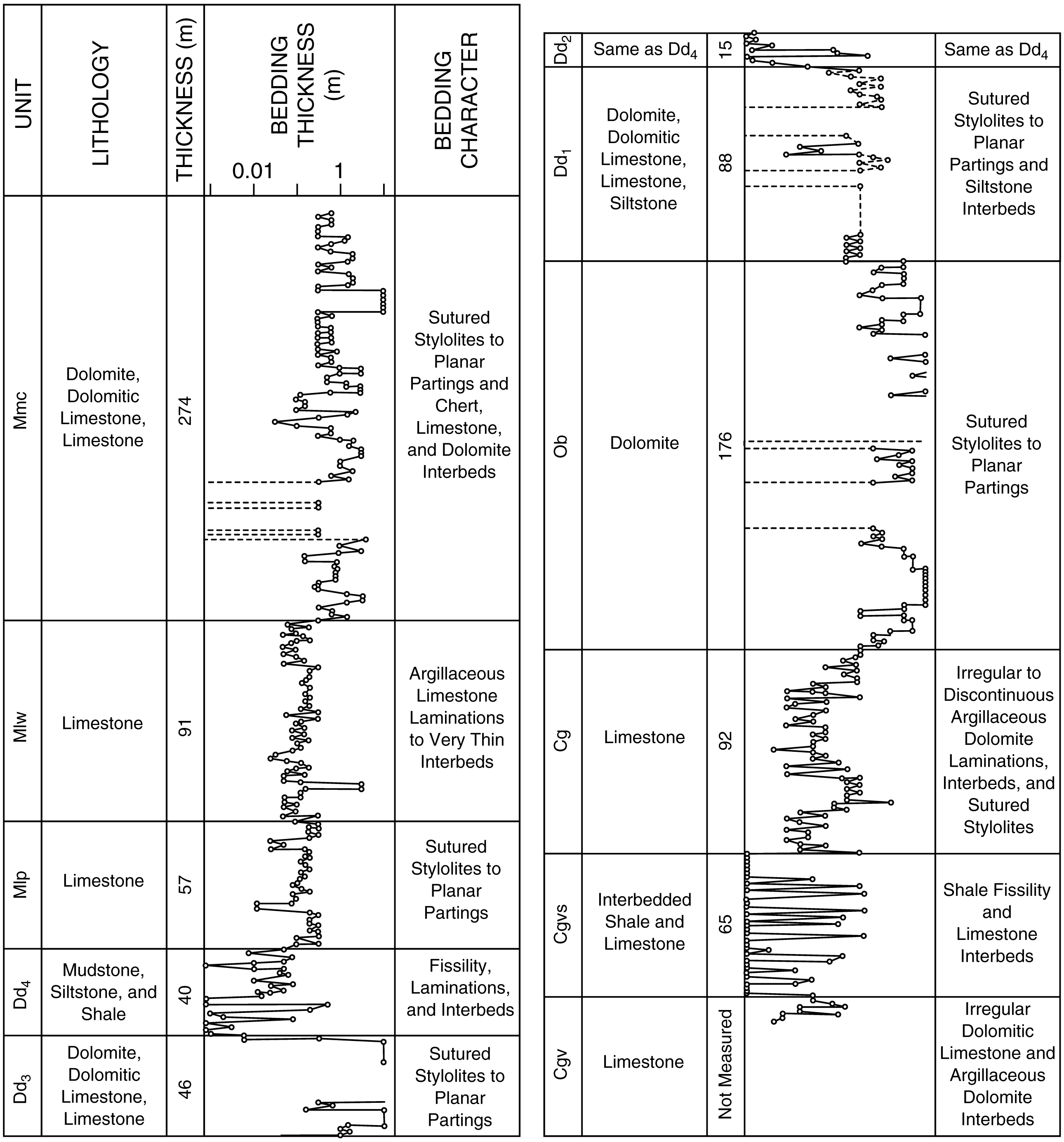

Fig. 3. Lithology, bedding thickness and character of bedding of the Paleozoic section in the Haystack Peak area.

interfaces; in order of increasing anisotropy these are sutured contacts, planar partings, and contrasting lithologic interbeds. Each unit is assigned a value from one to three in order of increasing anisotropy for each of the three parameters, which are totaled to give a qualitative strength anisotropy rating (Fig. 4).

The mechanical property characterization of the lower Paleozoic section identifies two main load bearing members or struts, the Bighorn Dolomite and Mission Canyon Formation, that have high strength, low relative ductility, and relatively low friction coefficients (Fig. 4). The struts consist of homogeneous, thin-bedded limestone at the base and more heterogeneous, thick-bedded dolomite or dolomitic limestone at the top. Each strut is underlain by a rock package that displays an overall downward decrease in bedding thickness and strength, and a downward increase in relative ductility and degree of anisotropy. Based on these data, i.e. intrinsic rock properties, the lower Paleozoic section can be divided into two similar mechanical units, each having a relatively incompetent lower section (Gros

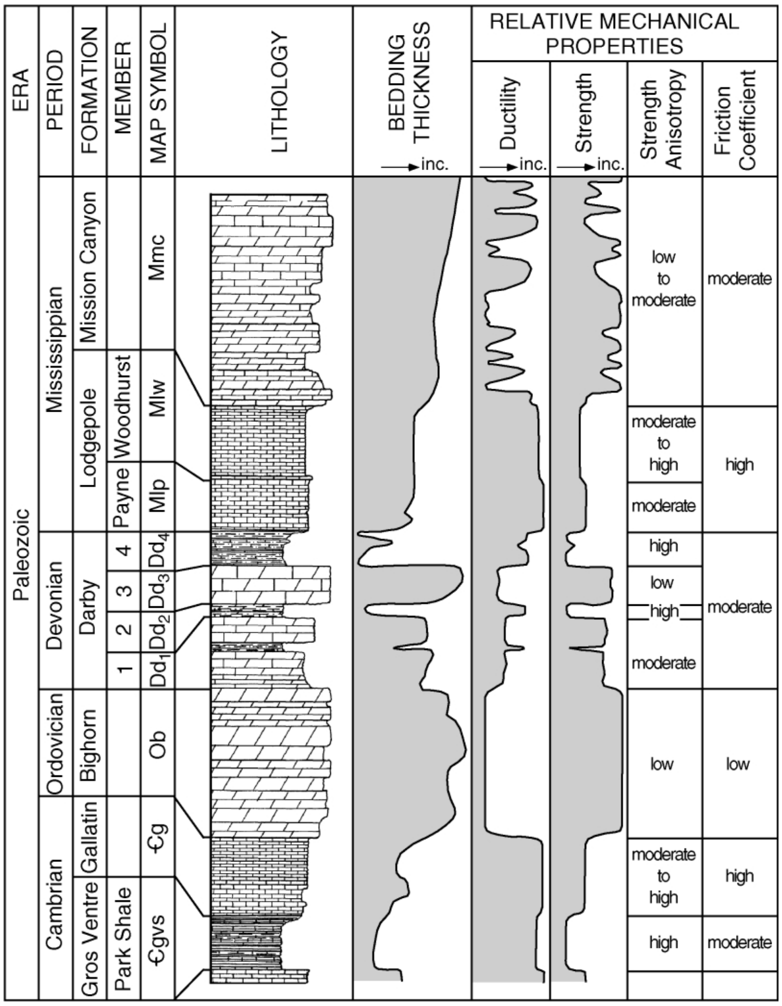

Fig. 4. Characterization of the mechanical properties of the Paleozoic section in the study area.

Ventre Formation, and unit #4 of Darby Formation) and competent upper section (Gallatin/Bighorn/lower Darby Formations, and Lodgepole/Mission Canyon Formations).

4. Structure in vicinity of Haystack Peak

The study area was mapped at a scale of 1:12,000 on enlargements of the Man Peak and Thayne East U.S.G.S. topographic sheets. The complete map (1:24,000) is available as an electronic supplement (plate 1 in Chester, 2002; see 'Electronic Supplements' on the journal homepage: http://www.elsevier.com/locate/jsg); a simplified map is presented in Fig. 5. Area balanced and restored cross-sections were prepared according to accepted principles (e.g. Dahlstrom, 1969; Elliot, 1976; Mitra, 1992). Map data were projected onto vertical sections parallel to average local fold axis orientation (Figs. 6 and 7). Color versions of the cross-sections (1:32,000) and restored sections (1:48,000) also are available as electronic supplements (plates 2 and 3, respectively, in Chester, 2002; see 'Electronic Supplements' on the journal homepage: http://www.elsevier.com/locate/jsg). Cross-section construction assumes deformation was approximately 2D and folding was by flexural-slip and flexural-flow mechanisms with localized thickening and thinning depending on stratigraphic unit and structural location.

The Stewart and Star thrust faults divide the Absaroka sheet into three main imbricate thrust sheets: the eastern imbricate sheet, situated between the Absaroka and Star thrust faults; the Star imbricate sheet between the Star and Stewart thrust faults; and the Stewart imbricate sheet west of the Stewart thrust fault (Fig. 5; plate 1 in Chester, 2002; see 'Electronic Supplements' on the journal homepage: http://www.elsevier.com/locate/jsg). The Stewart and Star thrust faults have been mapped north of the study area (Schroeder, 1981; Lageson, 1986), and the Stewart system continues south to at least Grover (Fig. 2; Royse et al., 1975; Chester, 1996). The structure in the study area is dominated by two fault complexes that occur within the Star imbricate sheet, the Stewart passive roof duplex that is bounded on the western side by the Stewart thrust, and the Star fault

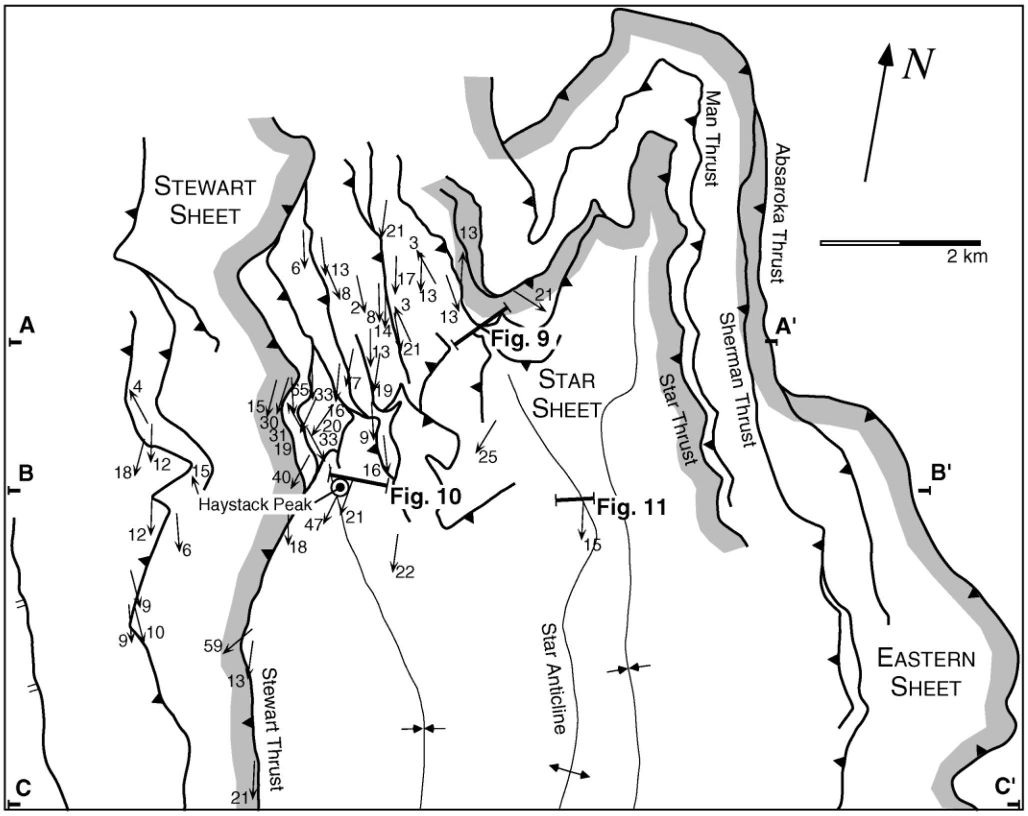

Fig. 5. Simplified structure map of study area showing major folds, thrust faults, key geographic features, and cross-section locations (Figs. 6 and 7). The Absaroka thrust sheet is subdivided into three sheets (eastern, Star, and Stewart imbricate sheets), defined by the surface traces of the major imbricate thrust faults (shaded on the hanging wall side). The locations of cliff exposures discussed in the text are indicated by figure number. Arrows represent trend and plunge of mesoscopic folds. The complete 1:24,000 geologic map is available as an electronic supplement (plate 1 in Chester, 2002; see 'electronic Supplements' on the journal's homepage: http://www.elsevier.com/locate/jsg).

complex that is bounded on the east by the Star thrust (Fig. 6).

4.1. Folds

The two main folds in this region are referred to as the Stewart and Star anticlines as they are cored by the Stewart and Star thrust faults, respectively (Fig. 6; plate 1 in Chester, 2002; see 'Electronic Supplements' on the journal homepage: http://www.elsevier.com/locate/jsg). Most folds are asymmetric to overturned with east-northeast vergence, consistent with the transport direction of the Absaroka thrust fault. The Star anticline is upright to overturned westward as is the Stewart anticline further south (Rubey, 1973; Chester, 1996). In detail, fold form varies for different rock units. Mesoscopic folds in the Gros Ventre and Gallatin Formations display relatively rounded hinges and locally approach concentric geometries. The degree of openness varies with intensity of deformation. In tightly folded regions shales display crenulation cleavage, particularly in fold hinges, and locally are thickened and thinned. The thin-bedded portions of the Bighorn Dolomite display some well-developed mesoscopic folds, but this unit primarily deformed by fracturing and faulting. Massive to thick-bedded dolomitic portions of the Darby Formation deformed by contractional faulting, similar to the Bighorn Dolomite, whereas thin-bedded siltstone and shale portions served as local detachment horizons and deformed by disharmonic folding.

Mesoscopic and macroscopic folds in the thin-bedded Lodgepole Formation display kink-style fold forms produced by flexural-slip. Fibrous calcite steps are displayed on many bedding surfaces, particularly in the Payne Member, indicating that solution-slip along bedding planes was an important folding mechanism. However, these features were not noted on all bedding surfaces within a fold, implying that the actual mechanical layer thickness was greater than the observed stratigraphic layer thickness. Kink-style folds also formed in the thick-bedded Mission Canyon Formation, but only at the macroscopic scale. The Mission Canyon Formation generally forms the largest amplitude, longest wavelength folds of the Paleozoic section.

All major and minor folds approach a cylindrical geometry in that poles to bedding planes lie close to a great circle in stereographic projection. The best-fit cylindrical fold axis to all bedding is 18°, 176° (Fig. 8a), and the mean orientation of mesoscopic fold axes is 24°, 175° (Fig. 8b). Subgroups of data for the Star and Stewart thrust sheets indicate a slight rotation in the best-fit cylindrical fold axis orientation between the two sheets

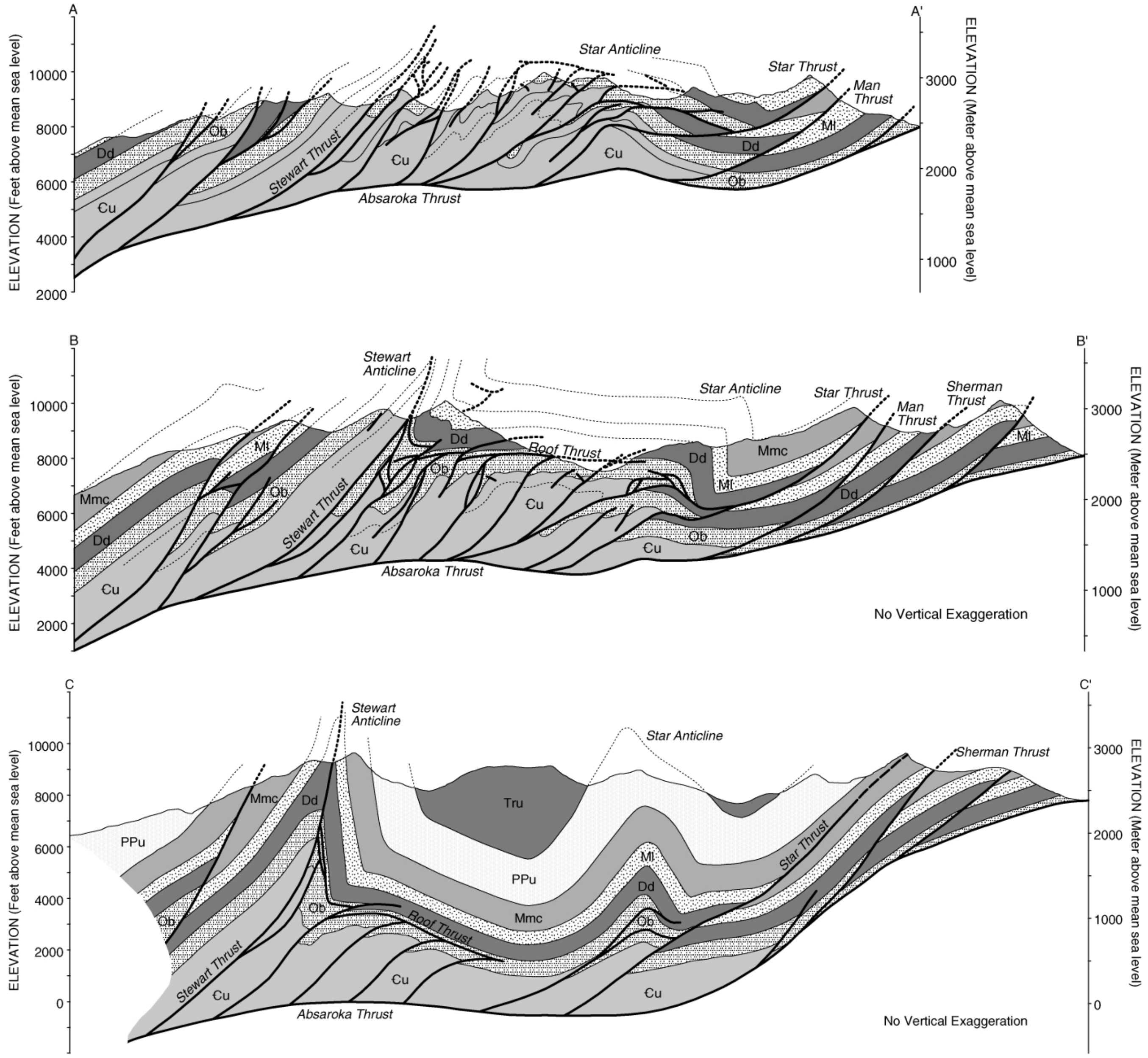

Fig. 6. Cross sections through the Absaroka thrust sheet along lines A, B, and C. Locations shown in Fig. 5.

(Chester, 1992). The steepest plunging folds are located within the Star sheet, and the most significant variation in fold axis orientation occurs in the vicinity of Haystack Peak, where fold axes plunge up to 47° and change trend by as much as 20° in a clockwise sense (Fig. 5; plate 1 in Chester, 2002; see 'Electronic Supplements' on the journal homepage: http://www.elsevier.com/locate/jsg). Similarly oriented fold axes occur directly to the northwest within horses of the Stewart thrust system.

4.2. Thrust faults

The trace of the Absaroka thrust fault, separating the Ordovician Bighorn Dolomite at the base of the hanging wall from Cretaceous strata in the footwall, lies at the eastern border of the range and is almost entirely covered by Quaternary deposits (Fig. 2; plate 1 in Chester, 2002; see 'Electronic Supplements' on the journal homepage: http://www.elsevier.com/location/jsg). The fault wraps around the base of Man Peak to form a reentrant to the northwest. The outcrop pattern at Man Peak indicates that the dip on the fault varies from horizontal to 10° southwest. Regionally, the outcrop trace of the Absaroka thrust essentially maintains a constant stratigraphic separation along the eastern margin of the Salt River Range south of Man Peak (Rubey, 1973; Woodward, 1987). However,

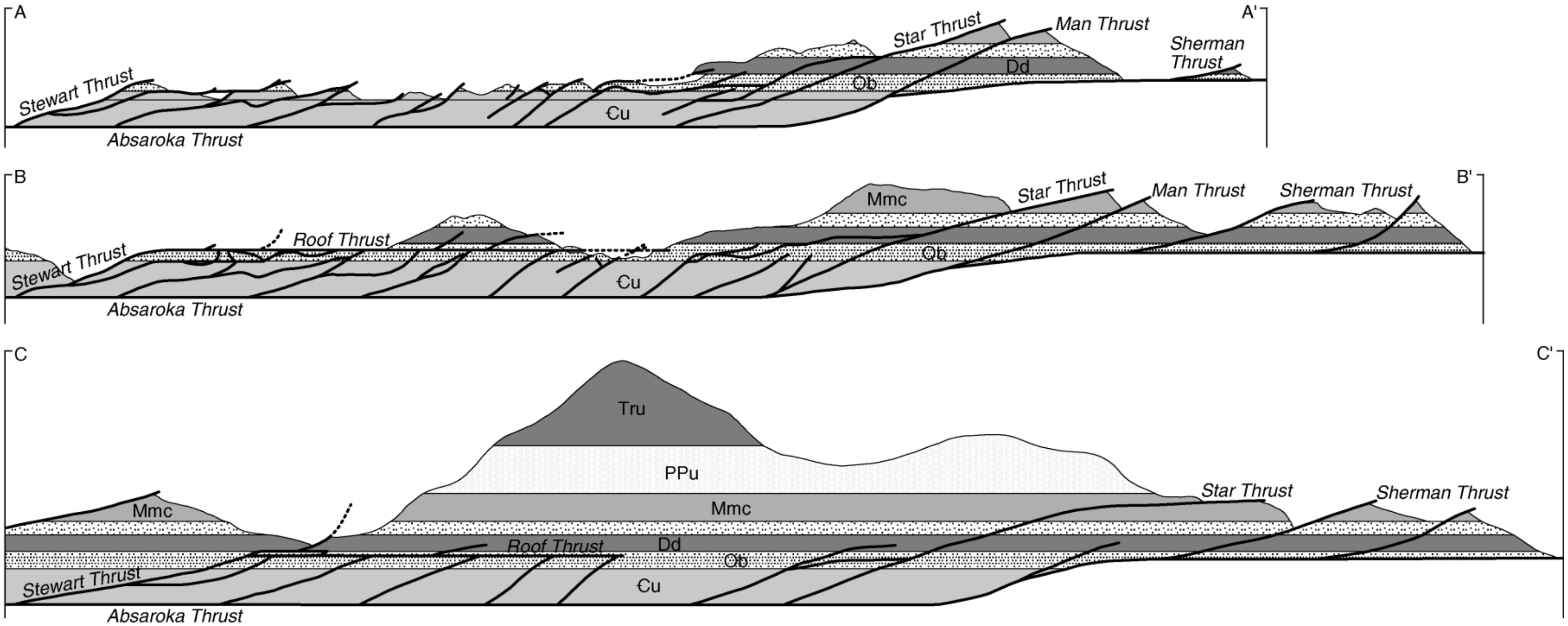

Fig. 7. Restoration of cross sections A-A′, B-B′, and C-C′ shown in Fig. 6.

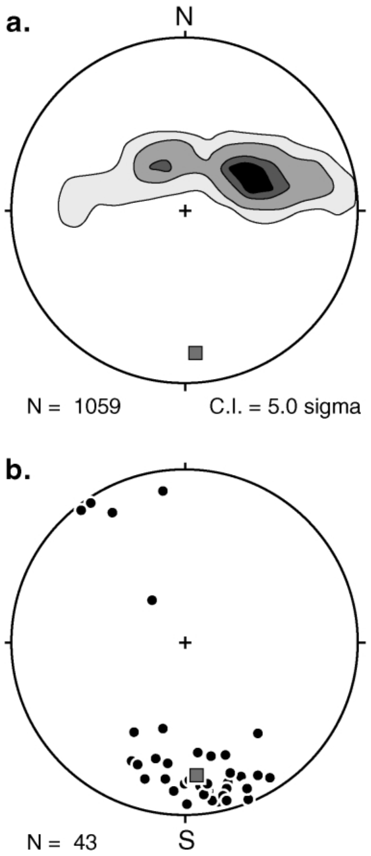

Fig. 8. Equal-area, lower-hemisphere projections on the horizontal plane with north at the top. (a) Kamb contour plot of poles to bedding. Best fit cylindrical fold axis is indicated by shaded square. (b) Axes of mesoscopic folds in the Stewart (10 measurements) and Star sheets (33 measurements). Mean fold axis is indicated by the shaded square.

north of Man Peak, stratigraphic separation varies because Cretaceous strata in the footwall are tightly folded (Rubey, 1973).

The Star thrust consists of a single fault at high structural levels (plate 1 in Chester, 2002; see 'Electronic Supplements' on the journal homepage: http://www.elsevier.com/locate/jsg). North and west of Man Peak, where lower structural levels are exposed, the Star thrust splays into two or more fault surfaces (Fig. 6). In the vicinity of Man Peak, the Star thrust dips 19–29° to the southwest. Along cross-section A–A′ the Star thrust has approximately 1.5 km of dip-slip at the surface, which decreases to approximately 1.2 km at the surface along cross section B–B′ (Fig. 6). This change represents an average decrease in dip-slip of approximately 130 m per 1 km of lateral horizontal length to the south.

The Stewart thrust consists of a single fault trace in the Stewart Peak area, having a stratigraphic separation of approximately 430 m, and is truncated to the northwest of Stewart Peak by the Grand Valley normal fault (Lageson, 1984). The dip on the Stewart thrust surface increases to the south, ranging from 49°, along the ridge of Haystack Peak to vertical in the vicinity of Strawberry Creek (Fig. 2; plate 1 in Chester, 2002; see 'Electronic Supplements' on the journal homepage: http://www.elsevier.com/locate/jsg). The maximum stratigraphic separation occurs just north of Haystack Peak where the Death Canyon Member of the Gros Ventre Formation and the Bighorn Dolomite are juxtaposed. South of Strawberry Creek the fault loses displacement so that the upper contact of the Bighorn Dolomite is not offset, although beds beneath the contact are faulted in the core of the fold.

4.3. Imbricate thrust sheets

4.3.1. Eastern thrust sheet

The eastern imbricate thrust sheet is cut by a forward-verging imbricate fan between the basal Absaroka and Star thrust surfaces (Figs. 5 and 6). The two larger imbricate faults within the eastern imbricate sheet are referred to as the Sherman and Man thrust faults, both of which are interpreted to merge with the Absaroka thrust at depth. Displacement across the Sherman thrust and a structurally lower, minor imbricate thrust fault are poorly constrained. The Sherman thrust has approximately 1.2 km of dip-slip in the vicinity of cross-section A–A′, and slip appears to decrease to the south. At Man Peak, excellent three-dimensional exposures of the Man thrust indicate approximately 400 m of dip-slip along section A–A′. The Man thrust also loses stratigraphic separation along its surface trace to the south, but hanging wall and footwall cut-offs are contained within the Mission Canyon Formation making estimation of stratigraphic separation difficult (plate 1 in Chester, 2002; see 'Electronic Supplements' on the journal homepage: http://www.elsevier.com/locate/jsg). An average decrease in dip-slip of approximately 80 m per 1 km of lateral horizontal length to the south was assumed for construction of cross-sections B–B′ and C–C′, which is within the range observed elsewhere within this region and for thrust faults in general (e.g. Nichol et al., 1996; Cartwright and Mansfield, 1998). Overall, the eastern imbricate sheet is characterized by tilted strata and fault-duplication but relatively little folding of strata.

4.3.2. Star thrust sheet

The Star imbricate thrust sheet displays the most intense and penetrative fault–fold deformation of all three imbricate sheets (Figs. 5 and 6). The transition in structural style from close-spaced faults and folds in the Cambrian–Ordovician units in the north to broad folds in the Mississippian units in the south is best displayed in this sheet. In the north, the Ordovician Bighorn Dolomite is cut by numerous imbricate faults that are underlain by tight folds in the Cambrian units (Fig. 9). At the scale of the map, the fold wavelength and fault spacing of the Cambrian–Ordovician units are on the order of 300 m (plate 1 in Chester, 2002; see 'Electronic Supplements' on the journal homepage: http://www.elsevier.com/locate/jsg). The overlying Devonian and Mississippian units, displayed to the

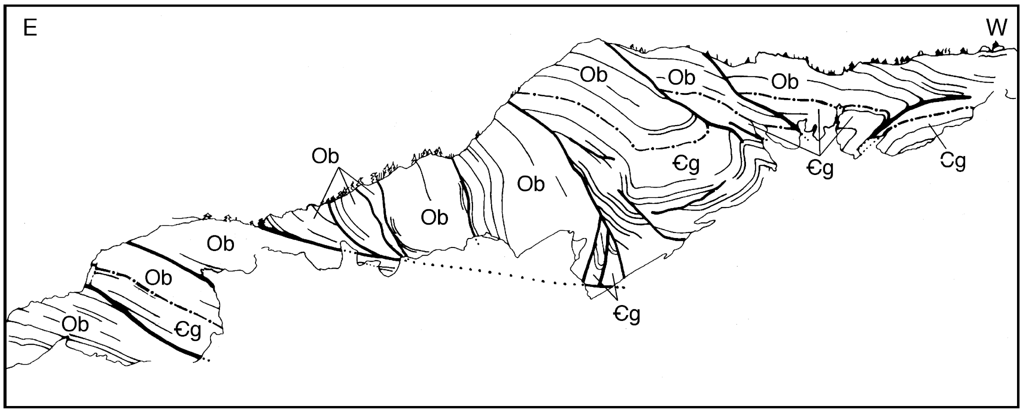

Fig. 9. Tracing from a photograph of the Gallatin–Bighorn contact displaying imbricate fault cut-off relationships and contrasting deformation style of each formation. View is to the south, vertical relief is approximately 305 m. Location indicated in Fig. 5.

south, show little evidence of shortening by imbrication or folding at the same scale displayed by older units immediately north. Rather, the dominant map-scale structures in the younger units of the Star sheet are the Star and Stewart folds, which are spaced approximately 2.4 km apart.

Detailed mapping demonstrates that most of the imbricate faults exposed in the north die out, shallow upward parallel to bedding, or join a roof thrust within and near the top of the Bighorn Dolomite (Fig. 6; plate 1 in Chester, 2002; see 'Electronic Supplements' on the journal homepage: http://www.elsevier.com/locate/jsg). The roof thrust forms the upper boundary of the Stewart passive roof duplex (Chester, 1996) that dominates the central and western portion of the Star imbricate sheet. The western boundary of the duplex is the Stewart thrust fault and the duplex forms the core of the Stewart anticline. Displacements on the imbricate faults within the duplex are on the order of hundreds of meters. Imbricate faults in the hinterland portion of the duplex display the greatest displacements. Collectively, imbrication and folding thickened strata in the duplex by up to 200%. Balancing constraints require significant hinterland-directed displacement of Devonian and Mississippian strata relative to Cambrian and Ordovician strata, which is interpreted to have occurred on the mapped roof thrust (Chester, 1996). The magnitude of hinterland-directed slip on the roof thrust increases with proximity to the Stewart thrust. Above the roof thrust, the Devonian and younger strata constitute a passive roof sequence that is relatively undeformed except near the hinge of the overturned syncline (Fig. 6). Two of the foreland-directed imbricate faults in the hinterland portion of the duplex offset the roof thrust just north of Haystack Peak. These offsets record the final displacements on the imbricate faults and termination of tectonic wedging in the passive roof duplex (Chester, 1996).

The stacked imbricate fault system in the Bighorn Dolomite projects below an overturned syncline in the footwall of the Stewart thrust fault exposed at Haystack Peak (Fig. 6; fig. 5 in Chester, 1996). The north-facing cliff exposure at Haystack Peak displays the contrasting style of deformation between the Darby and Lodgepole formations within the core of the overturned syncline (Fig. 10). The Darby Formation is thickened considerably by intraformational, disharmonic folding and faulting. Unit #3 of the Darby Formation is shortened by contraction faults that terminate upward and downward into a disharmonic system

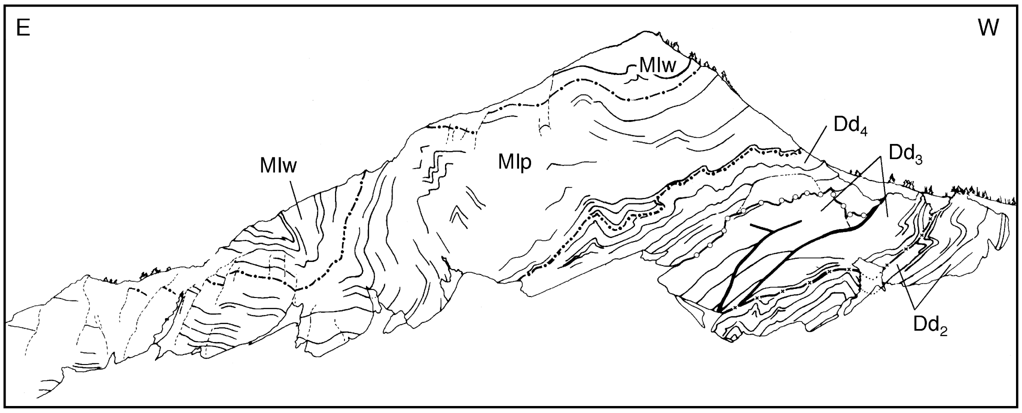

Fig. 10. Tracing from a photograph of Haystack Peak cliff exposure displaying contrasting deformational style of the Lodgepole and Darby Formations. View is to the south. Vertical relief is approximately 215 m. Location indicated in Fig. 5.

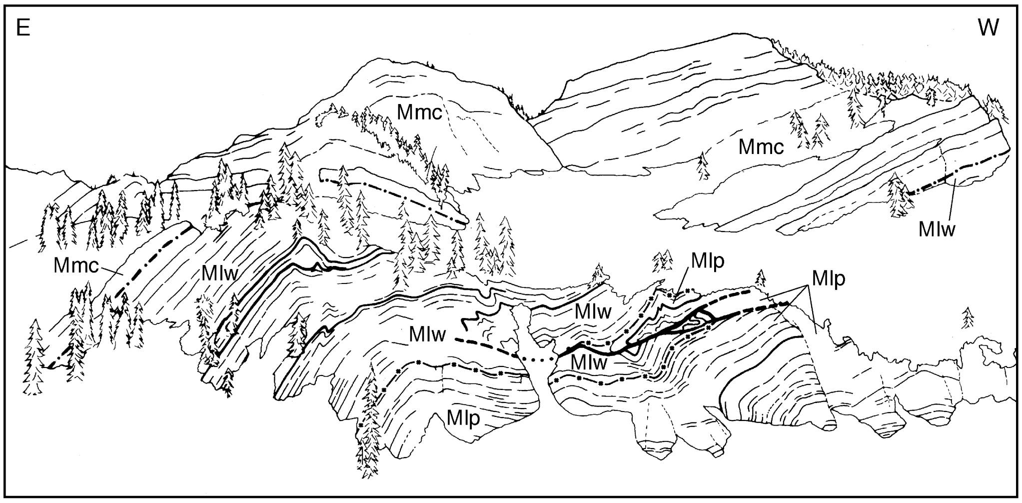

Fig. 11. Tracing from a photograph of the Lodgepole–Mission Canyon contact displaying contrasting deformational style of each formation. View is to the south. Vertical relief is approximately 125 m. Location indicated in Fig. 5.

of folds in the siltstone/shale units (#2 and #4). The overlying Lodgepole Formation displays small-wavelength, intraformational kink-style folds (Figs. 10 and 11) and thickening within the core of the large kink fold displayed in the Payne Member (Fig. 11).

South of Haystack Peak, on the north-facing canyon wall of Strawberry Creek, the western limb of the Stewart syncline is exposed in the Mission Canyon Formation (fig. 7 of Chester, 1996). This fold displays the large amplitude, long wavelength geometry, planar limbs, and sharp kink-style hinges characteristic of this unit. The synclinal hinge is extensively brecciated and numerous bedding planes display calcite fibers and slickenlines. These structures suggest that map-scale folding in the Mission Canyon Formation was by flexural-slip about a fixed hinge, where one limb accommodated most of the slip.

The Star fault complex in the eastern portion of the Star imbricate sheet is a single horse of Cambrian–Devonian strata that is cut by second-order imbricate faults and bounded on the west by the Star thrust (Fig. 6). The frontal imbricate fault of this complex does not display a footwall flat, but is folded so that the eastern portion of the horse is nearly horizontal. This complex has an overlapping ramp-anticline (Mitra, 1986) or simple antiformal stack (Boyer and Elliot, 1982) geometry. The Star thrust looses displacement to the south, and the overlapping ramp anticline or a related feature must continue in the subsurface to the south to core the Star anticline.

The surface geometry of folds along cross-section C–C′ (Fig. 6), fault displacements, and balancing constraints suggest that the Stewart duplex and Star fault complex diverge and become increasingly isolated southward. This may partly reflect the overall decrease in shortening within the Star thrust sheet from north to south.

4.3.3. Stewart thrust sheet

The Stewart imbricate thrust sheet is a gently dipping panel of strata cut by imbricate faults (Fig. 6). Overlying Mississippian rocks only display local folds at the current level of exposure, although the imbricate faults in this sheet may form the lower portions of a series of large fault–propagation folds that have since been eroded away. For the most part, strata within the imbricate fault stack are relatively less folded and less deformed in comparison with the Star thrust sheet, but are more folded than strata in the eastern imbricate sheet.

5. Discussion

5.1. Shortening estimates

Horizontal shortening is defined as the difference between present horizontal length (l_p) of a formation contact and original length (l_o) divided by original length (i.e. $[l_o - l_p]/l_o$), corrected for projection distortions. Magnitude of shortening was determined along cross-sections A–A′, B–B′, and C–C′ for the region between the Stewart and Sherman thrust faults because formation contacts between these two faults offered the greatest continuous exposures in the study area. Elsewhere, best estimates of shortening are shown in cross-sections based on projection of surface geology and balancing constraints.

Shortening of the lower Paleozoic section (Bighorn Dolomite and older strata) is well-constrained by surface data along cross-sections A–A′ and B–B′. Along cross-section A–A′ the best determination of shortening is afforded by the line-length of the Gallatin/Bighorn Formation contact, which records horizontal shortening between the Stewart and Man thrust faults of 54% (Fig. 6). A similar line-length determination is given by the upper contact of the Bighorn Dolomite along cross-section B–B′, which is within 5% of the horizontal shortening estimated using cross-sectional area (corrected for projection distortion) of the Bighorn Dolomite in section B–B′. The excess area relative to line length may be attributed to tectonic thickening of the Bighorn Dolomite by a combination of fracturing, cataclasis, mesoscale faulting, and folding at a scale that cannot be represented in the cross-sections but is observed at many localities in the field. If the structural domain between the Man and Sherman thrust faults is included in the line-length determination along cross-section A–A′, the overall magnitude of shortening decreases from 54% between the Stewart and Man thrust faults to 43% between the Stewart and Sherman thrust faults. This reflects the fact that the strata between the Man and Sherman thrust faults are shortened less, and that displacement on the Man thrust fault is relatively small.

Shortening of the upper Paleozoic section between the Stewart and Sherman thrust faults along cross-section C–C′ is 30%, based on the projected line-length of the Mission Canyon Formation contact (Fig. 6). For this determination, the contact is assumed to be smooth and not cut in the subsurface by imbricate faults other than the Star thrust. Thus, the actual magnitude of shortening is probably slightly greater than 30%, but still well below the shortening determined for the Bighorn Dolomite to the north.

All of these data illustrate that this portion of the Absaroka sheet is characterized by inhomogeneous internal shortening parallel to the transport direction. The Star thrust sheet experienced the greatest magnitude of shortening, and horizontal shortening varies along strike. The magnitudes of shortening reported show that that the north to south transition in structure, evident at the surface, may be attributed, in part, to a decrease in shortening from north to south over the study area.

5.2. Absaroka thrust fault

Over much of the Idaho–Wyoming portion of the thrust belt, surface, well, and seismic data indicate that the basal detachment lies within the Cambrian strata near the top of the Precambrian rocks (Royse et al., 1975; Dixon, 1982). Because the basal Cambrian shales are rarely exposed, the character of the detachment, exact location in the stratigraphic section, and thickness of the basal Cambrian section are relatively uncertain in the regions immediately surrounding the study area. The main basal detachment in the western portion of the Absaroka sheet (below the Star and Stewart sheets) is interpreted to lie in the Wolsey Shale Member of the Gros Ventre Formation, which places up to approximately 400 m of Cambrian strata in the hanging wall of the Absaroka sheet (Fig. 6).

In the Salt River Range, the Bighorn Dolomite forms the basal unit of the hanging wall of the Absaroka thrust along much of the outcrop trace (e.g. Rubey, 1973; Woodward, 1987). Mapping around the reentrant at Man Peak suggests that the Absaroka thrust cuts through the Bighorn Dolomite from west to east at a lower angle than the Cambrian strata to the west (plate 1 in Chester, 2002; see ‘Electronic Supplements’ on the journal homepage: http://www.elsevier.com/locate/jsg). These data imply that the Absaroka thrust forms a hanging wall ramp in the Cambrian near the location where the Absaroka and Man thrust faults merge in the subsurface (Fig. 6). These relations suggest that the Absaroka thrust followed the Ordovician horizon for some distance from west to east after cutting through the Cambrian section and prior to cutting through the Paleozoic strata along the Grand Valley ramp. Royse et al. (1975) display similar cut-off relationships in their cross-section interpretation through the Absaroka sheet south of the study area consistent with stratigraphic separation diagrams of Woodward (1987).

The depth of the Absaroka thrust increases to the south as indicated by the thickness of the faulted and folded strata in the hanging wall (Fig. 6). The apparent dip of the fault between cross-sections A–A′ and C–C′ averages approximately 11°. This dip is less than the average 18–24° plunge of folds in the hanging wall of the Absaroka sheet (Fig. 8). The steeper plunge of the folds probably reflects the decrease in shortening of the sheet from north to south. Surface geology and balancing constraints suggest, though do not necessarily require, that the Absaroka thrust is warped below the field area with a small undulation striking perpendicular to the transport direction, as well as an overall southerly dip (Fig. 6).

The dip of the Absaroka fault surface to the south has been noted by previous workers (e.g. Rubey, 1973; Royse et al., 1975; Lageson, 1980; Dixon, 1982; Woodward, 1987). Dixon (1982) interpreted the fault as an obliquely dipping surface under the field area, but predicted a greater depth to the fault than that predicted herein. Data from the Sun Prater Canyon well in the southeast portion of the Stewart Peak quadrangle demonstrate that the Absaroka fault surface is quite shallow to the north, and at about the same depth as depicted under the Star thrust sheet in cross-section A–A′ (Fig. 6; Lageson, 1984). This implies that the southerly dip of the Absaroka thrust largely occurs south of cross-section A–A′. A relatively horizontal fault surface between the Sun Prater Canyon well and cross-section A–A′, and a transverse dip between cross-sections A–A′ and C–C′ are consistent with topographic and stratigraphic relations exposed at the surface (Fig. 6; Rubey, 1973; Lageson, 1986) and with stratigraphic separation diagrams (Woodward, 1987). The depth shown in cross-section C–C′ (Fig. 6) is only slightly shallower than that indicated by Royse et al. (1975, plate I) farther south. If these subsurface interpretations are correct, then the transverse warp in the Absaroka thrust fault is fairly localized under the field area, largely occurring between cross-sections A–A′ and C–C′.

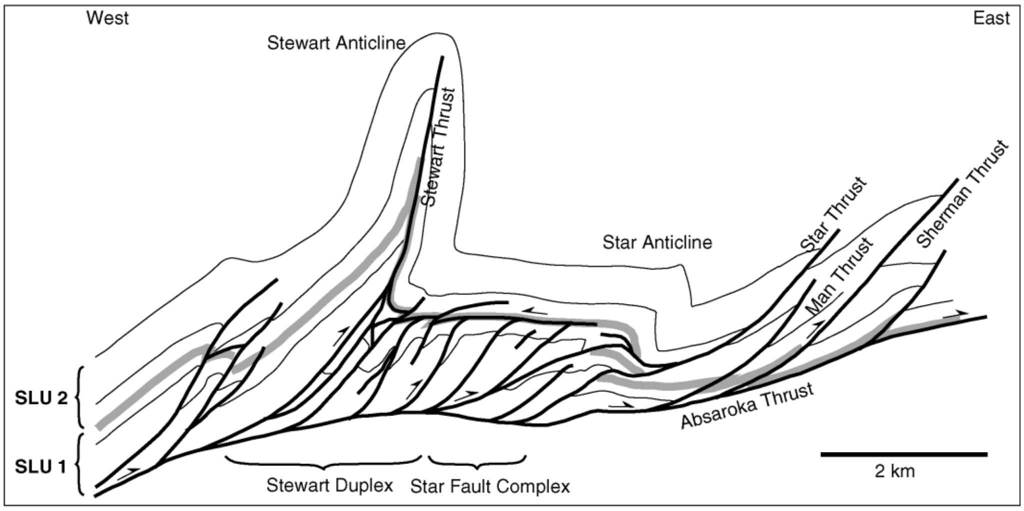

Fig. 12. Schematic cross-section parallel to B–B′ (Fig. 6) showing location of boundary (shaded line) between the two main structural lithic units (SLU1 and SLU2) relative to the main structural features.

5.3. Structural lithic units, mechanical behavior, and response of multilayers

Previous studies have discussed competence contrasts of the Paleozoic, Mesozoic and Cretaceous strata, and style of deformation in the Idaho–Wyoming–northern Utah (IWU) salient (e.g. Rubey, 1973; Royse et al., 1975; Chester, 1987, 1992; Woodward, 1988, 1992; Woodward and Rutherford, 1989; Goff et al., 1996). At the regional scale, it has been suggested that the Cambrian through Ordovician strata were less competent than, and conformed to, the upper Paleozoic strut (e.g. Royse et al., 1975, plate I; Woodward, 1992; Goff et al., 1996). For strata in the northern Idaho–Wyoming salient, Woodward (1988, 1992) defined four structural lithic units: the lower Paleozoic, upper Paleozoic, lower Mesozoic, and Cretaceous units. He concluded that the upper Paleozoic unit controlled deformation within the major thrust sheets in the northernmost portion of the belt and that the lower Mesozoic unit was increasingly dominant to the south reflecting its increased thickness southward (Woodward, 1992).

To understand the style of deformation within the imbricate thrust sheets in the vicinity of Haystack Peak, the relation between deformation style, lithology, and stacking order of Paleozoic strata is considered in more detail. Important variations in structural style include the overall transition from imbricate faulting and duplex development in the Cambrian–Ordovician strata to broad folds in Mississippian and younger strata, and the inverted fault–fold transitions (i.e. inverted fault–propagation folds) evident at the Mission Canyon–Lodgepole and Bighorn Dolomite–Gallatin contacts (plate 1 in Chester, 2002; see 'Electronic Supplements' on the journal homepage: http://www.elsevier.com/locate/jsg). Four key points are discussed: (1) the Paleozoic strata in the Star and Stewart imbricate sheets can be broken into two main structural lithic units if magnitude of shortening is considered; (2) the boundary between the two structural lithic units is best defined by the roof thrust, which occurs in a relatively thick-bedded portion of the Bighorn Dolomite (Fig. 12); (3) when the two structural lithic units were stacked, inverted fault–propagation folds formed in the center of each unit; and (4) when the upper structural lithic unit was isolated, as in the eastern imbricate sheet, deformation was dominated by imbricate faulting with little associated folding and inverted fault–propagation folds are absent.

The structural lithic unit designation for the Star sheet is supported by the fact that spacing of imbricate faults and wavelength of folds within the Stewart duplex and Star fault complex are approximately one tenth the spacing observed in overlying strata. Consistent with the definition given by Currie et al. (1962) (Fig. 12), these differences identify the boundary between two main structural lithic units. Based on the Stewart duplex, the boundary is located at the passive roof thrust in the upper Bighorn Dolomite. The location of this boundary is different from that designated by Woodward (1992) on the basis of more regional considerations. The Stewart imbricate sheet appears to display a different structural style at the macroscopic scale, i.e. imbrication without much folding, suggesting that the same structural lithic unit boundary does not apply to this latter sheet. However, at the outcrop and map scale there is ample evidence of local complexity, detachment, and folding near this same boundary in the Stewart sheet (Fig. 6; plate 1 in Chester, 2002; see 'Electronic Supplements' on the journal homepage: http://www.elsevier.com/locate/jsg). As such, a structural boundary is evident in the Stewart sheet even though this sheet is shortened much less than the Star sheet. If the more youthful stage of fault–fold development and magnitude of shortening are considered, it is argued that the same structural lithic unit designation can apply to both sheets.

What governs the formation and style of deformation of structural lithic units in this region? It is clear from the mechanical properties of the Paleozoic strata (Fig. 4) that each structural lithic unit is characterized by a relatively weak, ductile, anisotropic lower section and a relatively strong, brittle, more isotropic upper section. Nonetheless, this similarity alone does not explain the formation of inverted fault–fold transitions observed within each of the structural lithic units because these transitions only appear to form when the two units are stacked. This observation suggests that the mechanical interaction between the units also was important. When stacked, as in the Star and Stewart sheets, the entire package forms a multilayer composed of alternating stiff and soft layers. This multilayer package lies above a weak and ductile substratum (Wosley Shale) underlain by a major decollement, and is overlain by the strong and brittle upper Paleozoic strut. It is this multilayer character and boundary conditions that promote fine-scale folding within the individual structural lithic units, and contribute to the upward transition from close- to wide-spaced faults and folds (e.g. Donath and Parker, 1964; Johnson, 1970).

The distinct structural style of the upper structural lithic unit in the eastern imbricate sheet reflects the different boundary conditions associated with the absence of the lower structural lithic unit. In the eastern sheet, the lower boundary condition is governed by a decollement within the strong and brittle Bighorn Dolomite, rather than by a weak, anisotropic multilayer (Fig. 12). The single structural lithic unit in combination with the overlying Paleozoic strut, lacks the ductility and ductility contrasts apparently necessary to promote folding and formation of inverted fault–fold transitions characteristic of the stacked system. Differences in structural style resulting from the presence or absence of a particular unit is consistent with Woodward and Rutherford's (1989) hypothesis that the proportion of different strata within thrust sheets of the Idaho–Wyoming–Utah salient influenced fold-wavelength and fault-spacing. This concept also is consistent with the concept of strut members, first introduced by Willis (1894), and since treated in more detail in theoretical and experimental considerations of folding multilayers (e.g. Currie et al., 1962; Biot, 1964; Johnson, 1970; Johnson and Fletcher, 1994).

It is note-worthy that the boundary between the two main structural lithic units, defined by the Stewart roof thrust, did not form in the thin-bedded shale of the Darby Formation, but instead formed in the thick-bedded Bighorn Dolomite (Fig. 4). On the basis of strength, ductility and layer thickness such a detachment may be hard to explain, but is consistent with earlier data documenting major detachments in competent dolostones (e.g. Rubey, 1973; Burchfiel et al., 1982; Lamerson, 1982; Coleman and Lopez, 1986; Woodward, 1992). An excellent local example of a dolostone detachment is the hanging wall flat of the Absaroka thrust under much of the Salt River Range (Rubey, 1973). The existence of a detachment in dolostone suggests that a parameter(s) in addition to strength and ductility must play a critical role in dictating where detachments form. Burchfiel et al. (1982) proposed that strong decollement foreland thrusts, such as the Keystone–Muddy Mountain–Glendale and Contact–Red Spring–North Buffington–Morman thrust systems developed in dolostones because these highly competent units acted as stress guides concentrating horizontal stresses within them. Specifically how the horizontal stresses lead to decollement development was not addressed and the mechanical problem of explaining their existence was left unanswered.

As shown in the mechanical characterization of Paleozoic strata, a distinct mechanical property of dolostone, relative to the other lithologies, is relatively low frictional strength (Fig. 4). Laboratory experiments of frictional sliding show that dolostone has a low coefficient of friction relative to other sedimentary rocks (e.g. Handin, 1969; Logan et al., 1972). I propose that under shallow crustal conditions the shear strength for frictional sliding along a continuous bedding horizon within a massively bedded section of dolostone is much less than for sliding in other lithologies, and less than the strength of intact dolostone for shear across the layers.

In contrast with the hypothesis of Burchfiel et al. (1982), I suggest that the maximum compressive stress within the highly competent dolostone is not layer-parallel because such a stress state would result in low shear stress along bedding horizons and promote shear failure across bedding. Instead, the maximum compressive stress should be inclined to the foreland (e.g. Chapple, 1978) and frictional sliding along pre-existing bedding surfaces should be favored. Under the conditions of deformation in the Absaroka sheet, the frictional strength of the dolostone along a major bedding plane need only be less relative to that of the nearby shale or siltstone strata to grow into a decollement. Apparently the difference in frictional strength was significant enough to dictate the location of the roof thrust of the Stewart passive roof duplex, as well as the location of other significant detachments observed within dolostone horizons.

5.4. Kinematic interpretation

The truncated geometry of some Cretaceous folds suggests that Cretaceous strata presently in the footwall of the Absaroka thrust fault were folded, at least to some degree, before or during the formation of the Absaroka thrust fault (Fig. 13; Royse et al., 1975; Lageson, 1986; Mcbride and Dolberg, 1990; see also Woodward, 1987). This period of folding may have been associated with the formation and movement on the Murphy–Firetrail thrust system. Within the hanging wall of the Absaroka thust fault, shortening relations constrain the relative timing of imbrication and folding in the Star imbricate sheet, but not in the Stewart and eastern sheets.

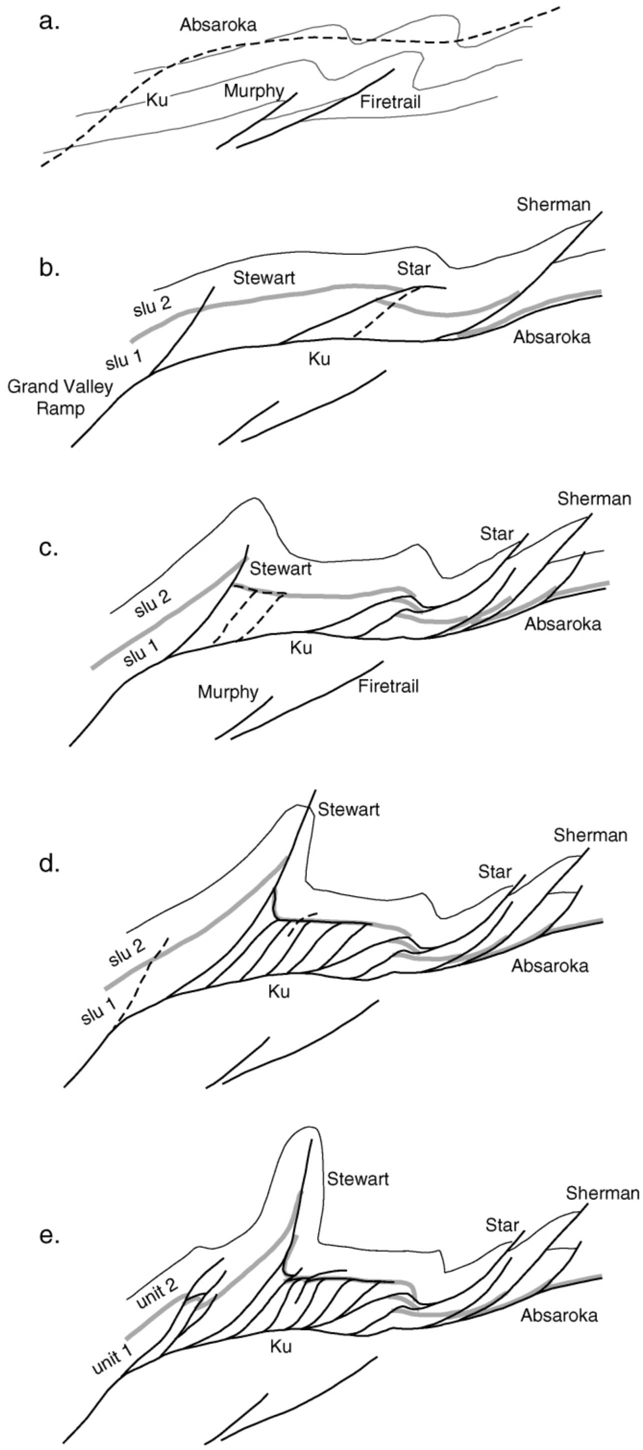

Fig. 13. Inferred sequence of deformation of the Absaroka thrust sheet parallel to cross-section B–B′ (Fig. 6). (a) Folding and faulting of Cretaceous units by the Murphy and Firetrail thrust faults prior to propagation of the Absaroka thrust. (b) Formation of the major imbricate thrust faults through break-back imbrication on the upper flat of the Grand Valley ramp. (c) Growth of the Star fault complex through footwall imbrication and initiation of the Stewart duplex. (d) Growth of the Stewart duplex through footwall imbrication and eastward extension of the backthrust. (e) Final shortening of the Stewart anticline after locking of the backthrust and imbrication in the Stewart sheet to produce present geometry.

5.4.1. Star fault complex

Folding and imbricate faulting in the vicinity of Haystack Peak were concurrent as faults are folded and folds are cut by faults. The westernmost imbricate of the Star complex cuts and offsets the overturned limb of an anticline–syncline pair near the Cambrian–Ordovician contact (Fig. 6). The local down-cutting of the fault at this locality suggests that some folding proceeded or accompanied fault-propagation. Subsequent translation of the fold in the hanging wall and duplication of strata produced a modified fault–bend fold (Fig. 6). This interpretation is different from the idealized fault–propagation or detachment fold interpretations offered by Jamison (1992), but much like the sequence envisioned by Berger and Johnson (1980) and Jamison (1987). Both imbricate faults of the Star complex appear folded at the level of the Cambrian through Ordovician strata, with the upper imbricate displaying the steepest foreland dip. This characteristic suggests that the more forward imbricate is younger and that the Star complex developed by break-forward imbrication. Balancing constraints and the geometry of the Absaroka thrust around the reentrant at Man Peak suggest that the Absaroka thrust may be locally warped into an antiform below the Star complex (Fig. 6). The antiform is similar in geometry to the overlying folded faults of the Star duplex. If correct, this relationship implies that the warping of the Absaroka thrust could have been contemporaneous with at least the latest stages of Star complex development and with shortening of the Absaroka sheet as a whole (Fig. 13). The warping may have been related to reactivation or continued movement on the underlying Murphy–Firetrail thrust system, consistent with suggestions of Royse et al. (1975) and Lageson (1984).

5.4.2. Stewart passive roof duplex

The Stewart thrust fault may have formed contemporaneous with or following the formation of the forward imbricate fault of the Star complex (Fig. 13). Development of the passive roof duplex occurred in the footwall of the Stewart thrust fault, below the forward limb of the overlying Stewart Anticline (Chester, 1996). Tectonic wedging allowed the Cambrian–Ordovician strata to shorten through fault duplication and folding, as Devonian and younger strata shortened through hinterland-directed displacement on the backthrust, amplification of the overlying Stewart anticline, and rotation and steepening of the Stewart thrust. Duplex formation within the tectonic wedge is interpreted to have occurred through forward-breaking imbrication, but with continued displacement on all imbricates throughout the period of wedge growth (Fig. 13). Continued movement on existing imbricate faults would tend to produce greater displacement on the more hindward imbricate faults relative to the more forward faults, as is observed in the field (plate 1 in Chester, 2002, see 'Electronic Supplements' on the journal homepage: http:www.elsevier.com/locate/jsg). In addition, such a movement history would produce forward growth and thickening of the wedge, consistent with the basic elements of wedge mechanics (e.g. Chapple, 1978). It is noted, however, that the simultaneous formation of imbricates, similar to that suggested by Cruikshank et al. (1991), cannot be ruled out.

The Cambrian–Ordovician contact within the duplex is folded and cut by footwall imbricates of the duplex. In addition, the footwall slice of the westernmost imbricate fault of the system contains a small anticline (plate 1 in Chester, 2002; see 'Electronic Supplements' on the journal homepage: http://www.elsevier.com/locate/jsg). These secondary structures are compatible with fault propagation along the axial surfaces of folds or through the frontal limbs of fault–propagation folds, similar to the character of the main structure, and provide evidence that folding within the Stewart duplex both proceeded faulting and occurred contemporaneously with fault growth.

Final shortening of the Star imbricate sheet was accommodated by the propagation of two hindward imbricate faults of the Stewart duplex across the roof thrust into overlying Devonian and younger strata (Fig. 13). Offset of the Darby Formation across these faults is much less than the total displacement on both faults at deeper structural levels, implying that offset of the Darby Formation occurred relatively late and that most displacement on the imbricate thrust faults was transferred to the roof thrust earlier. The late-stage propagation across the roof thrust produced secondary fault–propagation folds in overlying strata as observed on the north cliff face of Haystack Peak (Fig. 10). The late-stage offset of the roof thrust may have been associated with locking of the roof thrust and indicates termination of growth of the intercutaneous wedge (Chester, 1996).

5.5. Cause of imbrication and duplex development in light of theoretical models

The actual timing of hanging wall imbrication relative to formation of the Absaroka thrust cannot be stated definitively. If the major imbricate faults of the Absaroka thrust sheet (Stewart, Star, and Sherman) represent break-forward imbrication, then the Stewart duplex and Star system would have formed prior to translation of the Absaroka thrust sheet past the Grand Valley ramp. If so, these systems would have been carried up the ramp passively and transported to the present location. The Stewart and Star complexes then could represent either local structural complexities of unknown cause formed at a deeper structural level, or the characteristic pervasive style of deformation of the Absaroka sheet. The entire Absaroka sheet, however, is not shortened by imbrication to the extent displayed in the study area. In fact, regional subsurface interpretations of the major thrust sheets composing the Salient display extensive imbrication only on the upper footwall-flats of major frontal ramps (e.g. Royse et al., 1975; Dixon, 1982). This observation is difficult to explain by any model other than break-back imbrication on the upper footwall-flats of large frontal ramps (Fig. 13). This interpretation is consistent with Coogan's (1992) study of synorogenic deposits in the southern portion of the belt. Coogan (1992) showed that late-stage shortening and reactivation of large thrust faults, including the Absaroka, was accomplished by propagation of trailing ramp segments of faults across their hanging walls and overlying growth of anticlines.

Mechanical models of the deformation of thrust sheets translating over ramps indicate that regions above footwall flats adjacent to ramp-flat corners are most favorable for brittle faulting (e.g. Kilsdonk and Fletcher, 1989; Erickson and Jamison, 1995; Jamison, 1996; Chester and Fletcher, 1997; Strayer and Hudleston, 1997). It is in these areas that the ramp geometry produces high deviatoric stresses and low mean compressive stresses in the hanging wall. The mechanical models predict that similar stress states develop at both the lower and upper footwall ramp-flat corners. However, the absolute magnitude of the mean compressive stress most likely is greater at the lower ramp-flat corner of a large ramp due to the greater overburden. The greater mean compressive stress magnitude above the lower ramp-flat corner would tend to inhibit faulting at this location relative to the upper flat. Nucleation of major imbricate faults at or just past an upper ramp-flat corner as the thrust sheet translated past the ramp, as suggested by the mechanical models, would result in a break-back sequence of imbrication on the upper footwall flat.

The mechanical models alone, however, cannot explain why imbricate fans develop on some upper footwall flats and duplexes form on others. In a general sense, the formation of imbricate faults and duplexes within a thrust sheet represents a change in the mode of deformation from forward translation of the thrust sheet to internal shortening of the hanging wall. Changes in the mode of deformation have been attributed to an increase in the ratio of the resistance to forward translation of a sheet relative to internal hanging wall strength (Woodward et al., 1988; Chester et al., 1991; Strayer and Hudleston, 1997).

An increase in the resistance to forward translation of a sheet relative to internal hanging wall strength can be triggered by a change in boundary conditions, fold geometry, or mechanical properties of the thrust sheet (e.g. Berger and Johnson, 1980; Chester et al., 1991; Couzens and Wiltschko, 1996). Mitra (1986) suggests that the formation of hanging wall duplexes provides a mechanism of transferring slip to stratigraphically higher detachments when there is resistance to slip on the basal thrust fault. Couzens and Wiltschko (1996) hypothesize that the formation of passive roof duplexes at mountain fronts may be triggered by changes in the mechanical properties of a thrust sheet through the addition of syntectonic sedimentary strata. Dunne and Ferrill (1988) assumed that backthrusting associated with a passive roof duplex required that the cover was pinned to the thrust system immediately beyond the leading branch or tip-line of the active imbricate fault. Pinning represents a very high resistance to forward translation. The stratigraphic pinch-out of an incompetent glide horizon or presence of fault plane irregularities along the basal fault surface also may cause a change in mode of deformation (e.g. Gwinn, 1964; Mitra, 1986; Chester et al., 1991).

If imbrication of the Absaroka thrust sheet reflects a change in resistance to forward translation, such a change could have been related to several processes that have been suggested as possible causes of the Stewart Peak culmination. These include impingement of the thrust sheet on a preexisting basement uplift or warp (e.g. Blackstone, 1979; Lageson, 1984; Craddock et al., 1988; Kraig et al., 1988) or the introduction of an underlying fault plane irregularity introduced by motion on footwall imbricate faults (Lageson, 1984).

If movement on the underlying Murphy–Firetrail thrust system occurred during late-stage motion on the Absaroka thrust fault, then overlying features such as the Star and Absaroka thrust faults would become folded (Fig. 13). Folding would generate irregularities in the fault planes that may have contributed to terminating the growth of the Star complex, locking of the Absaroka thrust fault below the Star complex, and initiating the formation of the Stewart duplex. In this sense, the formation of the Stewart duplex could reflect a change from hanging wall translation and fault–bend folding on the Star and Absaroka thrust systems to internal shortening in the hindward portion of the sheet caused by an increase in the resistance to forward translation.

Lageson (1984) suggested that the Murphy, Firetrail, and Absaroka thrust faults comprise a large-scale duplex system north of the study area, with Absaroka thrust fault forming the roof fault. It has been suggested that duplex development at deep structural levels may trigger duplex formation at higher structural levels, when the underlying duplex system locks (e.g. Yin and Kelty, 1991). If this were true in the study area, then the Star complex and Stewart duplex may be related to the Firetrail–Murphy–Absaroka duplex.

Considering changes in mode of deformation within individual thrust sheets as a consequence of changes in resistance to translation and strength is analogous to the analysis of thrust belts in terms of critically tapered deforming wedges (e.g. Chapple, 1978; Davis et al., 1983; DeCelles and Mitra, 1995). Wedge theory is based on the concept that forward translation is allowed only when a critical taper is achieved via internal deformation (e.g. Mitra and Sussman, 1997). Episodes of internal wedge deformation may be a consequence of changes in wedge taper due to erosion, changes in wedge strength due to incorporation of more sedimentary strata with time, changes in decollement strength resulting from a weakening or hardening process, changes in orientation of layering, or changes in strength and ductility of each lithologic unit that result from strain softening or hardening processes (e.g. DeCelles and Mitra, 1995). Thus the late-stage imbrication and duplex development seen in the Absaroka thrust sheet may reflect a period of tectonic thickening necessary to reestablish critical taper and allow subsequent forward translation and growth of the regional thrust wedge.

6. Conclusions

The transversely dipping structure of the Absaroka thrust sheet, excellent exposures, and topographic relief allowed geometric and kinematic subsurface interpretations to be developed for this portion of the sheet. Map relations indicate that the later-stages of emplacement of the Absaroka sheet were associated with the development of two large fault-cored anticlines, the Star fault complex and Stewart duplex, significant hinterland-directed thrusting along a dolomite detachment horizon, out-of-sequence imbricate faulting, and distinct vertical transitions in structural style.

The main fault–fold structures in the Absaroka sheet formed in a foreland to hinterland sequence largely in response to the movement of the sheet over the Grand Valley dip ramp. In contrast, imbricate faults within the main fault–fold structures formed in a break-forward sequence as shortening and overlying fold amplitude increased. Overall, the initiation and termination of duplexing and faulting in the cores of the folds are related to the progressive growth, tightening, and locking of anticlines.

The transition in structural style from close-spaced faults and folds in the lower Paleozoic strata to wide-spaced, broad open folds in the younger strata reflect magnitude of shortening, lithologic contrasts, and stacking order of lithologies. Based on the variation in deformation style, the Paleozoic section may be divided into two structural lithic units. In the easternmost and structurally lowest domain (eastern imbricate sheet) where only the upper structural lithic unit is present, shortening was achieved by imbricate fan development. In domains where both structural lithic units are present, large magnitude shortening was achieved by duplex development in the lower unit and large amplitude, long wavelength folding in the upper unit.

The distinction of structural lithic units in this region is facilitated by the fact that portions of the sheet display relatively large magnitudes of shortening. Comparison of the structural lithic units and mechanical characterization of strata suggests that the structural lithic units do not solely reflect strength and ductility, but also the degree of mechanical anisotropy and frictional strength. What units combine to form a structural lithic unit will depend on the properties of the unit and the boundary conditions. On the basis of this study, structural lithic unit identification may be helpful to palinspastic reconstructions as it provides a useful framework for subsurface interpretation. However, in order to understand the behavior of each structural lithic unit, knowledge of the mechanical properties and boundary conditions are necessary.

The hinterland progression of imbricate faulting associated with movement over the upper footwall flat is consistent with predictions of mechanical models of the ramp regions of thrust faults. The vertical change in style within the Absaroka thrust sheet, from imbricate faulting to passive roof duplexing, is consistent with the suggestion that the sheet experienced a change in the resistance to translation relative to internal shortening over time. This change produced an overall thickening of the sheet, and serves as an example of a relatively late-stage mechanism by which a thrust wedge can maintain a critical taper.

Acknowledgements

Early field work for this study was supported by grants from Chevron USA, Amoco Production Company and ARCO and is gratefully acknowledged. I thank J. Morse for logistical support in the field and F. Chester for valuable field assistance. Thorough and thoughtful reviews by F. Chester and journal referees N. Woodward and A. Yonkee greatly improved this manuscript.

References

Armstrong, F.C., Oriel, S.S., 1965. Tectonic development of Idaho–Wyoming thrust belt. American Association of Petroleum Geologists Bulletin 49, 1847–1866.

Atkinson, B.K., 1984. Subcritical crack growth in geological materials. Journal of Geophysical Research 89, 4077–4114.

Berger, P., Johnson, A.M., 1980. First-order analysis of deformation of a thrust sheet moving over a ramp. Tectonophysics 70, T9–T24.

Biot, M.A., 1964. Theory of internal buckling of a confined multilayered structure. Bulletin of Geological Society of America 75, 563–568.

Biot, M.A., 1965a. Theory of viscous buckling and gravity instability of multilayers with large deformation. Bulletin of Geological Society of America 76, 371–378.

Biot, M.A., 1965b. Further development of internal buckling of multilayers. Bulletin of Geological Society of America 76, 833–840.

Blackstone, D.L., 1979. Geometry of the Prospect–Darby and LaBarge faults at their junction with the LaBarge Platform, Lincoln and Sublette Counties, Wyoming. Geological Survey Wyoming Report of Investigations 18, 34pp.

Boyer, S.E., Elliot, D., 1982. Thrust systems. American Association of Petroleum Geologists Bulletin 66, 1196–1230.

Budai, J.M., Wiltschko, D.V., 1987. Structural controls on syntectonic diagenesis within the Haystack Peak region of the Absaroka thrust sheet, Idaho–Wyoming–Utah thrust belt. Wyoming Geological Association 38th Annual Field Conference, Guidebook, pp. 55–68.

Budai, J.M., Lohmann, K.C., Wilson, J.L., 1987. Dolomitization of the Madison Group, Wyoming and Utah overthrust belt. American Association of Petroleum Geologists 71, 909–924.

Burchfiel, B.C., Wernicke, B., Willemin, J.H., Axen, G.J., Cameron, C.S., 1982. A new type of decollement thrusting. Science 300, 513–515.

Cartwright, J.A., Mansfield, C.S., 1998. Lateral displacement variation and lateral tip geometry of normal faults in the Canyonlands National Park, Utah. Journal of Structural Geology 20, 3–19.

Chapple, W.M., 1978. Mechanics of thin-skinned fold-and-thrust belts. Geological Society of America Bulletin 89, 1189–1198.

Chester, J.S., 1987. Mechanical stratigraphy of the Cambrian through Mississippian section in the Absaroka thrust sheet, Haystack Peak area, Wyoming. Geological Society of America Abstracts with Programs 19, 618.

Chester, J.S., 1992. Role of mechanical anisotropy in the internal evolution of a thrust sheet. Ph.D. thesis, Texas A & M University.

Chester, J.S., 1996. Geometry and kinematics of a passive-roof duplex in the interior of the Idaho–Wyoming–northern Utah thrust belt. Bulletin of Canadian Petroleum Geology 44, 363–374.

Chester, J.S., 2002. Geologic map and cross-sections of the Haystack Peak area, Salt River Range, Wyoming. http://www.elsevier.com/inca/publications/store/5/3/9/.

Chester, J.S., Fletcher, R.C., 1997. Stress distribution and failure in anisotropic rock near a bend on a weak fault. Journal of Geophysical Research 102, 693–708.

Chester, J.S., Logan, J.M., Spang, J.H., 1991. Influence of layering and boundary conditions on fault-bend and fault-propagation folding. Geological Society of America Bulletin 103, 1059–1072.

Cobbold, P.R., Cosgrove, J.W., Summers, J.M., 1971. Development of internal structures in deformed anisotropic rocks. Tectonophysics 12, 23–53.

Coleman, J.L. Jr, Lopez, J.A., 1986. Dolomite decollements—exception or rule? American Association of Petroleum Geologists, Bulletin 70, 576.

Coogan, J.C., 1992. Structural evolution of piggyback basins in the Wyoming–Idaho–Utah thrust belt. In: Link, P.K., Kentz, M.A., Platt, L.B. (Eds.), Regional Geology of Eastern Idaho and Western Wyoming. Geological Society of America Memoir 179, pp. 55–81.

Corbett, K., Friedman, M., Spang, J., 1987. Fracture development and mechanical stratigraphy of Austin Chalk, Texas. American Association of Petroleum Geologists Bulletin 71, 17–28.

Couzens, B.A., Wiltschko, D.V., 1996. The control of mechanical stratigraphy on the formation of triangle zones. Bulletin of Canadian Petroleum Geologists 44, 165–179.

Craddock, J.P., Kopania, A.A., Wiltschko, D.V., 1988. Interaction between the northern Idaho–Wyoming thrust belt and bounding basement blocks, central western Wyoming. In: Schmidt, C.J., Perry, W.J., Jr. (Eds.), Interaction of the Rocky Mountain Foreland and the Cordilleran Thrust Belt. Geological Society of America Memoir 171, pp. 333–351.

Cruikshank, K.M., Zhao, G., Johnson, A.M., 1991. Duplex structures connecting fault segments in Entrada Sandstone. Journal of Structural Geology 13, 1185–1196.

Currie, J.B., Patnode, H.W., Trump, R.P., 1962. Development of folds in sedimentary strata. Geological Society of America Bulletin 73, 655–674.

Dahlstrom, C.D.A., 1969. Balanced cross-sections. Canadian Journal of Earth Sciences 6, 743–757.

Davis, D., Suppe, J., Dahlen, F.A., 1983. Mechanics of fold-and-thrust belts and accretionary wedges. Journal of Geophysical Research 88, 1153–1172.

DeCelles, P.G., Mitra, G., 1995. History of the Sevier orogenic wedge in terms of critical taper models, northeast Utah and southwest Wyoming. Geological Society of America Bulletin 107, 454–462.

Dixon, J., 1982. Regional structural synthesis. Wyoming salient of western Wyoming overthrust belt. American Association of Petroleum Geologists Bulletin 60, 1560–1580.

Donath, F.A., Parker, R.B., 1964. Folds and folding. Geological Society of America Bulletin 75, 45–62.

Douglas, R., 1950. Callum Creek, Langford Creek and Gap map areas, Alberta, Canada. Geological Survey of Canada Memoir 255, 1–124.

Dunne, W.M., Ferrill, D.A., 1988. Blind thrust systems. Geology 16, 33–36.

Elison, M.W., 1991. Intracontinental contraction in western North America: continuity and episodicity. Geological Society of America Bulletin 103, 1226–1238.

Elliot, D., 1976. The motion of thrust sheets. Journal of Geophysical Research 81, 949–963.

Erickson, S.G., Jamison, W.R., 1995. Viscous-plastic finite-element models of fault-bend folds. Journal of Structural Geology 17, 561–573.

Erickson, S.G., Strayer, L.M., Suppe, J., 2001. Initiation and reactivation of faults during movement over a thrust faults ramp: numerical mechanical models. Journal of Structural Geology 23, 11–23.

Fischer, M.P., Jackson, P.B., 1999. Stratigraphic controls on deformation patterns in fault-related folds: a detachment fold example from the Sierra Madre Oriental, northeast Mexico. Journal of Structural Geology 21, 613–633.

Goff, D.F., Wiltschko, D.V., Fletcher, R.C., 1996. Decollement folding as a mechanism for thrust-ramp spacing. Journal of Geophysical Research 101, 11,341–11,352.

Gross, M.R., 1995. Fracture partitioning: failure mode as a function of lithology in the Monterey Formation of coastal California. Geological Society of America Bulletin 107, 779–792.

Gross, M.R., Gutierrez-Alonso, G., Bai, T., Wacker, M.A., Collingsworth, K.B., Behl, R.J., 1997. Influence of mechanical stratigraphy and kinematics on fault scaling relations. Journal of Structural Geology 19, 171–183.

Gwinn, V.E., 1964. Thin-skinned tectonics in the plateau and northwest Valley and Ridge provinces of central Appalachians. Geological Society of America Bulletin 75, 863–900.

Handin, J., 1969. On the Coulomb–Mohr failure criterion. Journal of Geophysical Research 74, 5343–5348.

Handin, J., Hager, R.V. Jr, Friedman, M., Feather, J.N., 1963. Experimental deformation of sedimentary rocks under confining pressure: pore pressure tests. American Association of Petroleum Geologists Bulletin 45, 717–755.

Heard, H.C., 1963. Effect of large changes in strain rate in the experimental deformation of Yule Marble. Journal of Geology 71, 162–195.

Jamison, W.R., 1987. Geometric analysis of fold development in overthrust terranes. Journal of Structural Geology 9, 207–219..

Jamison, W.R., 1992. Stress controls on fold thrust style. In: McClay, K.R., (Ed.), Thrust Tectonics, Chapman & Hall, pp. 155–164.

Jamison, W.R., 1996. Bulletin of Canadian Petroleum Geology 44, 180–194.

Johnson, A.M., 1970. Physical Processes in Geology, Freeman Cooper and Company, 577pp.

Johnson, A.M., 1977. Styles of Folding, Elsevier, 406pp.

Johnson, A.M., Fletcher, R.C., 1994. Folding of Viscous Layers: Mechanical Analysis and Interpretation of Structures in Deformed Rock, Columbia University Press, 461pp.

Kilsdonk, B., Fletcher, R.C., 1989. An analytical model of hanging-wall and footwall deformation at ramps on normal and thrust faults. Tectonophysics 163, 153–168.

Kraig, D.H., Wiltschko, D.V., Spang, J.H., 1988. The Interaction of the Moxa Arch (LaBarge Platform) with the Cordilleran thrust belt, south of Snider Basin, southwestern Wyoming. In: Schmidt, C.J., Perry, W.J. (Eds.), Interaction of the Rocky Mountain Foreland and the Cordilleran Thrust Belt. Geological Society of America Memoir, 171pp.

Lageson, D.R., 1978. Petrography of selected rock samples and discussion of structural fabric, northern Salt River Range, Lincoln County, Wyoming. Geological Survey of Wyoming, Preliminary Report 17.

Lageson, D.R., 1980. Structural geology of the Stewart Peak quadrangle, Lincoln County, Wyoming, and the adjacent parts of the Idaho–Wyoming Thrust Belt. Ph.D. thesis, University of Wyoming.

Lageson, D.R., 1984. Structural geology of the Stewart Peak Culmination, Idaho–Wyoming Thrust Belt. American Association of Petroleum Geologists Bulletin 68, 401–416.

Lageson, D.R., 1986. Geologic map of the Stewart Peak Quadrangle, Lincoln County, Wyoming: Geological Survey of Wyoming Map series 22.

Lamerson, P.R., 1982. The Fossil Basin and its relation to the Absaroka thrust system, Wyoming and Utah. In: Powers, R.B., (Ed.), Geologic Studies of the Cordilleran Thrust Belt, Rocky Mountain Association of Geologists, pp. 279–340.

Latham, J.-P., 1985a. The influence of nonlinear material properties and bending resistance upon the development of internal structures. Journal of Structural Geology 7, 225–236.

Latham, J.-P., 1985b. A numerical investigation and geological discussion of the relationship between folding, kinking and faulting. Journal of Structural Geology 7, 237–249.

Logan, J.M., Iwasaki, T., Friedman, M., Kling, S. A., 1972. Experimental investigation of sliding friction in multilithologic specimens. In: Pincus, H. (Ed.), Geologic Factors in Rapid Excavation. Geological Society America, Engineering Case History 9, pp. 55–67.

Mcbride, B.C., Dolberg, D.M., 1990. Re-evaluation of the Stewart Peak culmination and the relationship between the St. John's and Absaroka thrust faults. Geological Society of America Abstracts with Programs 22, 37.

Mitra, S., 1986. Duplex structures and imbricate thrust systems: geometry, structural position, and hydrocarbon potential. American Association of Petroleum Geologists Bulletin 70, 1087–1112.

Mitra, S., 1992. Balanced structural interpretations in fold and thrust belts. In: Mitra, S. and Fisher, G.W., (Eds), Structural Geology of Fold and Thrust Belts. Johns Hopkins University Press, Baltimore.

Mitra, G., Sussman, A.J., 1997. Structural evolution of connecting splay duplexes and their implications for critical taper: an example based on geometry and kinematics of the Canyon Range culmination, Sevier Belt, central Utah. Journal of Structural Geology 19, 503–522.

Nichol, A., Watterson, J., Walsh, J.J., Childs, C., 1996. The shapes, major axis orientations and displacement patterns of fault surfaces. Journal Structural Geology 18, 235–248.

Raleigh, C.B., Griggs, D., 1963. Effect of the toe in the mechanics overthrust faulting. Geological Society of America Bulletin 74, 819–830.

Ramberg, H., 1970. Folding of laterally compressed multilayers in the field of gravity I. Physics of the Earth and Planetary Interiors 2, 203–232.

Rich, J.L., 1934. Mechanisms of low-angle overthrust faulting as illustrated by Cumberland thrust block, Virginia, Kentucky, and Tennessee. American Association of Petroleum Geologists Bulletin 18, 1584–1596.

Royse, F., Jr., Warner, W.A., Reese, D.L., 1975. Thrust belt structural geometry and related stratigraphic problems-Wyoming–Idaho–northern Utah. In: Rocky Mountain Association of Geologists, Symposium on Deep Drilling Frontiers of the Central Rocky Mountains, pp. 41–54.

Rubey, W.W., 1973. Geologic map of the Afton quadrangle and parts of the Big Piney quadrangle, Lincoln and Sublette Counties, Wyoming. U.S. Geological Survey. Misc. Inv. Series Map I-686, scale 1:65,000.

Rutter, E.H., 1976. The kinetics of rock deformation by pressure solution. Philosophical Transactions of the Royal Society of London, Series A: Mathematical and Physical Sciences 283, 203–219.

Rutter, E.H., 1983. Pressure solution in nature, theory and experiment. Journal of the Geological Society of London 140, 725–740.

Schirmer, T.W., 1988. Structural analysis using thrust-fault hanging-wall sequence diagrams: Ogden duplex, Wasatch Range, Utah. Bulletin of American Petroleum Geologists 72, 573–585.

Schroeder, M.L., 1981. Geologic map of the Deer Creek Quadrangle, Lincoln County, Wyoming. U.S. Geological Survey Geologic Quadrangle Map GQ-1551, scale 1:24,000.

Strayer, L.M., Hudleston, P.J., 1997. Numerical modeling of fold initiation at thrust ramps. Journal of Structural Geology 19, 551–556.

Wanless, H.R., Belknap, R.L., Foster, H., 1955. Paleozoic and Mesozoic rocks of Gros Ventre, Teton, Hoback and Snake River Ranges, Wyoming. Geological Society of America Memoir 63, 106.

Webel, S., 1987. Significance of backthrusting in the Rocky Mountain thrust belt. Wyoming Geological Association 38th Annual Field Conference, Guidebook, pp. 37–53.

Willis, B., 1894. Mechanics of Appalachian structure. United States Geological Survey 13th Annual Report, pp. 211–281.

Wiltschko, D.V., 1979. A mechanical model for thrust sheet deformation at a ramp. Journal of Geophysical Research 84, 1091–1104.

Wiltschko, D.V., Dorr, J.A. Jr, 1983. Timing of deformation in overthrust belt and foreland of Idaho, Wyoming and Utah. American Association of Petroleum Geologists Bulletin 67, 1304–1322.

Woodward, N.B., 1986. Thrust fault geometry of the Snake River Range, Idaho and Wyoming. Geological Society of America Bulletin 97, 178–193.

Woodward, N.B., 1987. Stratigraphic separation diagrams and thrust belt structural analysis. Wyoming Geological Association 38th Annual Field Conference, Guidebook, pp. 69–77.

Woodward, N.B., 1988. Primary controls on thrust sheet geometries. In: Schmidt, C.J., Perry, W.J. (Eds.), Interaction of the Rocky Mountain Foreland and the Cordilleran Thrust Belt. Geological Society of America Memoir 171, pp. 353–366.

Woodward, N.B., 1992. Deformation styles and geometric evolution of some Idaho–Wyoming thrust belt structures. In: Mitra, S., Fisher, G.W. (Eds.), Structural Geology of Fold and Thrust Belts, Johns Hopkins University Press, pp. 191–206.

Woodward, N.B., Rutherford, E. Jr, 1989. Structural lithic units in external orogenic zones. Tectonophysics 158, 247–267.

Woodward, N.B., Wojtal, S., Paul, J.B., Zadins, Z.Z., 1988. Partitioning of deformation within several external thrust zones of the Appalachian Orogen. Journal of Geology, 96, 351–361.

Yin, A., Kelty, T.K., 1991. Structural evolution of the Lewis plate in Glacier National Park, Montana: implications for regional tectonic development. Geological Society of America Bulletin 103, 1073–1089.

Yonkee, W.A., 1992. Basement-cover relations, Sevier orogenic belt, northern Utah. Bulletin of the Geological Society of America 104, 280–322.